

RESEARCH ARTICLE

Climatology, variability, and trends in near-surface wind speeds over the North Atlantic and Europe during 1979–2018 based on ERA5

Terhi K. Laurila¹  | Victoria A. Sinclair²  | Hilppa Gregow¹ 

¹Weather and Climate Change Impact Research, Finnish Meteorological Institute, Helsinki, Finland

²Institute for Atmospheric and Earth System Research/Physics, Faculty of Science, University of Helsinki, Helsinki, Finland

Correspondence

Terhi K. Laurila, Weather and Climate Change Impact Research, Finnish Meteorological Institute, Helsinki, Finland.

Email: terhi.laurila@fmi.fi

Funding information

Academy of Finland, Grant/Award Numbers: 303951, 307331; ERA4CS WINDSURFER; MONITUHO; Satakunnan Rahasto, Grant/Award Number: 75181580

Abstract

This study presents the monthly 10-m wind speed climatology, decadal variability and possible trends in the North Atlantic and Europe from ERA5 reanalysis from 1979 to 2018 and investigates the physical reasons for the decadal variability. Additionally, temporal time series are examined in three locations: the central North Atlantic, Finland and Iberian Peninsula. The 40-year mean and the 98th percentile wind speeds emphasize a distinct land-sea contrast and a seasonal variation with the strongest winds over the ocean and during winter. The strongest winds and the highest variability are associated with the storm tracks and local wind phenomena such as the mistral. The extremeness of the winds is examined with an extreme wind factor (the 98th percentile divided by mean wind speeds) which in all months is higher in southern Europe than in northern Europe. Mostly no linear trends in 10-m wind speeds are identified in the three locations but large annual and decadal variability is evident. The decadal 10-m wind speeds were stronger than average in the 1990s in northern Europe and in the 1980s and 2010s in southern Europe. These decadal changes were largely explained by the positioning of the jet stream and storm tracks and the strength of the north–south pressure gradient in the North Atlantic. The 10-m winds have a positive correlation with the North Atlantic Oscillation in the central North Atlantic and Finland on annual scales and during cold season months and a negative correlation in Iberian Peninsula mostly from July to March. The Atlantic Multi-decadal Oscillation has a moderate negative correlation with the winds in the central North Atlantic but no correlation in Finland and Iberian Peninsula. Overall, our results emphasize that while linear trends in wind speeds may show a general long-term trend, more information on the changes is obtained by analysing long-term variability.

KEYWORDS

climate, climatology, ERA5, trends, variability, wind speed

This is an open access article under the terms of the Creative Commons Attribution License, which permits use, distribution and reproduction in any medium, provided the original work is properly cited.

© 2020 The Authors. *International Journal of Climatology* published by John Wiley & Sons Ltd on behalf of Royal Meteorological Society.

1 | INTRODUCTION

The knowledge of long-term climatology and variability of 10-m wind speeds is valuable for meteorologists and climate scientists. For example, forecasters need to know the mean wind climate in order to estimate the local extremeness in wind forecasts, and climate model simulations are typically compared and validated against the long-term mean climate. The near-surface winds have an important role in advection and surface fluxes to transfer heat and moisture horizontally and vertically between the atmosphere and the surface. Moreover, information of the near-surface wind speed climate and variability is essential for industries that are dependant or affected by winds such as wind energy, forestry and insurance. For example, Gregow *et al.* (2016) highlight the energy sector's desire for higher resolution and accurate wind datasets.

In addition to global and regional wind atlases, reanalyses are a relevant source for wind assessments. Reanalysis systems provide a consistent analysis of the atmospheric state and aim to utilize observations as extensively as possible (Dee *et al.*, 2014). Such datasets are well suited to wind assessments due to their global coverage, homogeneous data and long time periods. Previous studies (e.g., Kaiser-Weiss *et al.*, 2015, 2019) have compared in-situ surface wind observations to reanalysis and, in general, it has been shown that the frequency distributions of mean wind speeds are well captured in reanalysis. The long-term wind speed variability and/or trends have been studied with many different reanalyses—e.g., ERA-Interim, MERRA-2, and JRA-55 (Torralba *et al.*, 2017), NOAA-20CR (Bett *et al.*, 2013) and ERA-40 (Kiss and Jánosi, 2008)—but not yet with the new ERA5 reanalysis (Hersbach *et al.*, 2020). The knowledge of the mean climate in ERA5 is needed since it will most likely be used as a basis to compare both historical runs and future projections from climate models (e.g., Priestley *et al.*, 2020). Furthermore, ERA5 has been found to outperform MERRA-2 in the wind power modelling (Olauson, 2018) and hence, ERA5 is likely to be used in many wind-related applications.

The long-term surface wind speeds over land have shown a decreasing trend, termed stilling, over the last few decades in 1979–2008 (Vautard *et al.*, 2010). However, a reversal in global stilling has been detected after 2010 (Zeng *et al.*, 2019). The timing of this reversal varies in different regions and in Europe, the turning point was obtained in 2003 (Zeng *et al.*, 2019). Vautard *et al.* (2010) found that 10–50% of the stilling can be explained by atmospheric circulation changes and 25–60% by an increase in surface roughness. Similarly, a recent review by Wu *et al.* (2018) summarizes that the long-term

terrestrial wind speed changes are caused by the driving forces (atmospheric circulation) and drag forces (surface friction such as land use and cover change and urbanization, and boundary layer conditions). However, since there are no sudden surface roughness changes in 2010 although a reversal was found, Zeng *et al.* (2019) suggest that the wind speed variability is mainly associated with the decadal variations in large-scale ocean-atmospheric circulations, such as the North Atlantic Oscillation (NAO) in Europe, the Pacific Decadal Oscillation in Asia and the Tropical Northern Atlantic Index in North America.

Previously, climatological studies of 10-m wind speeds (e.g., Bett *et al.*, 2013, 2017) have mainly concentrated on long-term linear trends and the variability has been examined over the whole time period with statistical measures (e.g., the standard deviation). Variations of the wind climate between different decades has received less attention and often the decadal variability can be determined from time series using techniques such as Gaussian low-pass filters (Azorin-Molina *et al.*, 2014; Minola *et al.*, 2016) or piecewise linear regression models (Zeng *et al.*, 2019). Such station-based time series studies have been examined separately in multiple European countries (e.g., Azorin-Molina *et al.*, 2014; Minola *et al.*, 2016; Laapas and Venäläinen, 2017, Zahradníček *et al.*, 2019). However, a decadal analysis over a larger domain would provide new information on the large-scale spatial patterns and their changes in each decade. Furthermore, the decadal analysis of 10-m wind speeds can then be compared to spatial and decadal patterns in other atmospheric variables, such as upper-level winds and mean sea level pressure, to study the reasons behind the decadal changes.

Longer range predictions of 10-m wind speeds on multiple time scales (months, years, decades) give value in long-term planning, adaptation and preparedness in societies and many sectors since extreme winds can cause diverse impacts, for example, uproot trees in forests (Gardiner *et al.*, 2010; Usbeck *et al.*, 2012; Gregow *et al.*, 2017) or generate high waves which impact coastlines and offshore infrastructure (Vose *et al.*, 2014). As long-term variations in 10-m wind speeds are influenced by changes in the atmospheric circulation, seasonal forecasts of near-surface winds are often based on indices that describe the large-scale atmospheric patterns (Scaife *et al.*, 2014). For the North Atlantic and Europe region, a commonly used index is the NAO which is a key source of seasonal predictability skill in many European regions (Scaife *et al.*, 2014). On decadal and climatological scales, the Atlantic Multi-decadal Oscillation (AMO) could possibly give some value since the periodical cycle of the AMO is around 70 years (Zhang *et al.*, 2019).

The first aim of this study is to present the wind speed climate in the North Atlantic and Europe based on ERA5 and to identify any long-term linear trends. In contrast to many earlier studies, we present monthly averages rather than seasonal or annual averages which likely suppress variability or disguise details. The second aim is to determine if there are decadal variations in the 10-m mean and extreme wind speeds. Since wind speed has a large year-to-year variability, and potentially long-term oscillations, the decadal analysis provides considerably more information than the linear trends. The third and final aim is to investigate physical reasons for possible wind speed changes on the decadal scale in the North Atlantic and Europe, which we do by examining whether 10-m wind speeds correlate with other atmospheric variables and climatic indices. The remainder of this paper is structured as follows. Section 2 describes the data and methods that we use, the wind speed climate is presented in Section 3 and wind speed variability and trends in Section 4. In Section 5 we investigate the physical reasons for the wind speed changes, and finally the conclusions are given in Section 6.

2 | DATA AND METHODS

2.1 | ERA5 reanalysis

ERA5 is the fifth generation atmospheric reanalysis from the European Centre for Medium Range Weather Forecasts (Hersbach *et al.*, 2020). ERA5 uses the Integrated Forecasting System (IFS, cycle 41r2) and includes atmosphere, land surface and ocean wave models. In addition to the improved data assimilation system compared to its predecessor ERA-Interim (Dee *et al.*, 2011), ERA5 has a higher spatial and temporal resolution. The horizontal resolution in ERA5 is approximately 31 km (TL639 in spectral space) and it has 137 vertical levels (from surface to around 80 km). The analysis and forecast fields are available hourly. Currently ERA5 covers the time period from 1979 onwards but is expected to finally be available from 1950.

In this study, we used 6-hourly data from 1979 to 2018 with 0.25° (~31 km) horizontal resolution. The variables we obtained are instantaneous 10-m and 300-hPa horizontal wind components and mean sea level pressure.

2.2 | NAO and AMO indices

The NAO (North Atlantic Oscillation) index describes the large-scale circulation pattern in the North Atlantic.

When NAO is positive, there is a larger than average pressure difference between the northern and southern Atlantic resulting in warmer, wetter and generally more stormy conditions in northern Europe (Hurrell, 1995). A traditional way to quantify the NAO is to calculate the pressure difference between Iceland and the Azores, however, a station-based method may not capture the large-scale spatial pattern and can be noisy. Hence, it is more common to use a principal component -based method to reduce these limitations. The NAO index used in this study is calculated by applying the Rotated Principal Component Analysis to the monthly standardized 500-hPa height anomalies which is produced by the Climate Prediction Center at the National Oceanic Atmospheric Administration (NOAA, 2020a).

The AMO (Atlantic Multi-decadal Oscillation) index describes the sea surface temperature (SST) variability in the North Atlantic. When AMO is in the positive phase, SSTs in the North Atlantic are warmer than on average. This affects Europe during summertime leading to wetter conditions over central and eastern Europe and drought conditions in parts of southern, western and Northern Europe (Ionita *et al.*, 2012). However, Yamamoto and Palter (2016) found that during winter the thermodynamic response of AMO to European weather is overruled by the dynamical response from NAO. In this study we use the AMO index calculated from the Kaplan SST dataset (Kaplan *et al.*, 1998) detrended and area-averaged over the Atlantic between 0 and 70°N (Enfield *et al.*, 2001; NOAA, 2020b).

2.3 | Diagnostics and trend analysis

In this study, we consider the wind climatology over the 40-year period (1979–2018). For each month, we calculated the mean (WS_{mean}), the 98th percentile (WS_{98}), standard deviation, and the extreme wind factor (EWF) from the 6-hourly winds, and we define

$$\text{EWF} = \frac{WS_{98}}{WS_{\text{mean}}}. \quad (1)$$

The standard deviation measures the variations in the mean climate whereas the EWF emphasizes how extreme the extreme winds are relative to the mean at each individual grid point. By definition, EWF must always exceed one as the 98th percentile wind speed is always greater than the mean wind. If the EWF is much larger than one the 98th percentile winds are much stronger than the mean winds implying that the wind speed distribution is wide with a large positive tail. In contrast, a EWF close to one indicates that the 98th percentile winds are not that

extreme compared to the mean and the wind speed distribution is narrow. Therefore, higher EWF values likely lead to more wind damage and impacts.

To examine the decadal variation, we divided the climatological period to four 10-year periods (1979–1988, 1989–1998, 1999–2008, 2009–2018) and calculated the 10-year means separately for each month. Hereinafter these time periods are referred to as 1980s, 1990s, 2000s and 2010s for clarity although the years do not exactly match the decades. The wind speed variation is analysed with relative anomalies (10-year mean value minus 40-year mean value divided by 40-year mean value) whereas the EWF variation is analysed relative to the climatological mean (10-year EWF minus 40-year mean wind speed). We present the monthly results from the cold season (September–February) and the other months are given in the Supporting Information (Figures S1–S4).

In addition to the monthly decadal variability in the North Atlantic and Europe domain, we analysed wind speed time series in more detail in three locations: in the central North Atlantic in the region with the strongest winds, and over land separately in northern and southern parts of Europe where we found opposite wind anomalies in many decades. More precisely, the chosen coordinates for the locations are the central North Atlantic (20–40°W, 45–60°N), Finland (20–30°E, 60–70°N) and Iberian Peninsula (0–9°W, 37–43°N) and the locations are shown as boxes in Figure 1. The time series were produced by first calculating a statistical value (mean, 98th percentile, maximum, standard deviation or EWF) at each grid point and then averaging the values over all grid points in each longitude–latitude box. Since the box over the central North Atlantic is bigger than the ones over Europe, the variability is smoother due to bigger area averaging.

To identify the temporal trends in the three boxes, we applied the Mann-Kendall test (Mann, 1945; Kendall, 1970) which can be used to test the statistical significance of the trends. The magnitude of the trends was determined from the Theil-Sen's slope estimator (Theil, 1950; Sen, 1968). Both the Mann-Kendall test and the Theil-Sen's slope are nonparametric and distribution-free methods. In addition to the trends, we correlated monthly and annual wind speed time series and NAO and AMO indices by using linear least-squares regression and the Wald test. Both the trends and correlations were tested at the significance level of 5% (p -value < 0.05).

To investigate the physical reasons, we first investigate the monthly correlation between 10-m and 300-hPa wind speeds (representative of the jet stream level) primarily to determine if the 300-hPa winds are a dominant reason for the 10-m wind speed spatial variability. The 10-m winds are harder to forecast, even at the very short lead times, than 300-hPa wind speeds. In addition,

climate models, which are run at coarse resolution, may not accurately capture the current 10-m wind speed climate or future changes. Therefore, by examining the correlation between 10-m and 300-hPa wind speeds, we test whether the 300-hPa wind speeds could be used as a proxy for 10-m winds on monthly scales which further could give potential for extended and longer range forecasting. Secondly, the decadal 10-m wind speed anomalies in February are examined in relation to anomalies of the 300-hPa wind speed, storm tracks and mean sea level pressure (MSLP) to further assess the physical reasons for the decadal variability. This month was chosen because the wind speed anomalies at the decadal scale were the largest in February (shown in Figure 6). Lastly, we investigate whether the temporal variability in 10-m wind speeds at the three locations is correlated with the NAO and AMO.

Storm tracks are commonly analysed with the Eulerian diagnostic of bandpass-filtering (Blackmon, 1976). In our study, we analysed the storm tracks by using the Eulerian measure to 6-hourly MSLP from 1979 to 2018 from ERA5. First, we detrended the MSLP data and then processed the data with 2–6 day bandpass filter. From the bandpass-filtered MSLP, we calculated the monthly standard deviation for the 10-year periods as well as the whole 40-year period.

3 | WIND SPEED CLIMATE

The monthly mean 10-m wind speed over the 40-year period (1979–2018) shows a clear land-sea gradient and a seasonal variation with the strongest winds over the ocean areas and during winter months (Figure 1). Over the North Atlantic, the strongest mean wind speeds during winter months exceed $12 \text{ m}\cdot\text{s}^{-1}$ whereas in July the highest monthly mean wind speeds are below $8 \text{ m}\cdot\text{s}^{-1}$. The area of strongest wind speeds over the North Atlantic between 10–50°W and 40–60°N is associated with the main North Atlantic storm track region (contours in Figure 1). During summer months, there is a noticeable area of low wind speeds over the southern North Atlantic between 20–40°W and 25–35°N. These calm winds at the horse latitudes are caused by the divergence between prevailing westerlies on the northern side and trade winds on the southern side.

Over land areas in Europe, the absolute mean wind speed difference between winter and summer months is not as high as over the ocean, mostly between 1 and $2 \text{ m}\cdot\text{s}^{-1}$ (Figure 1). However, the relative difference is similar with mean winds in winter being around 1.5 times stronger than in summer. There is a narrow band of higher wind speeds spreading horizontally over central

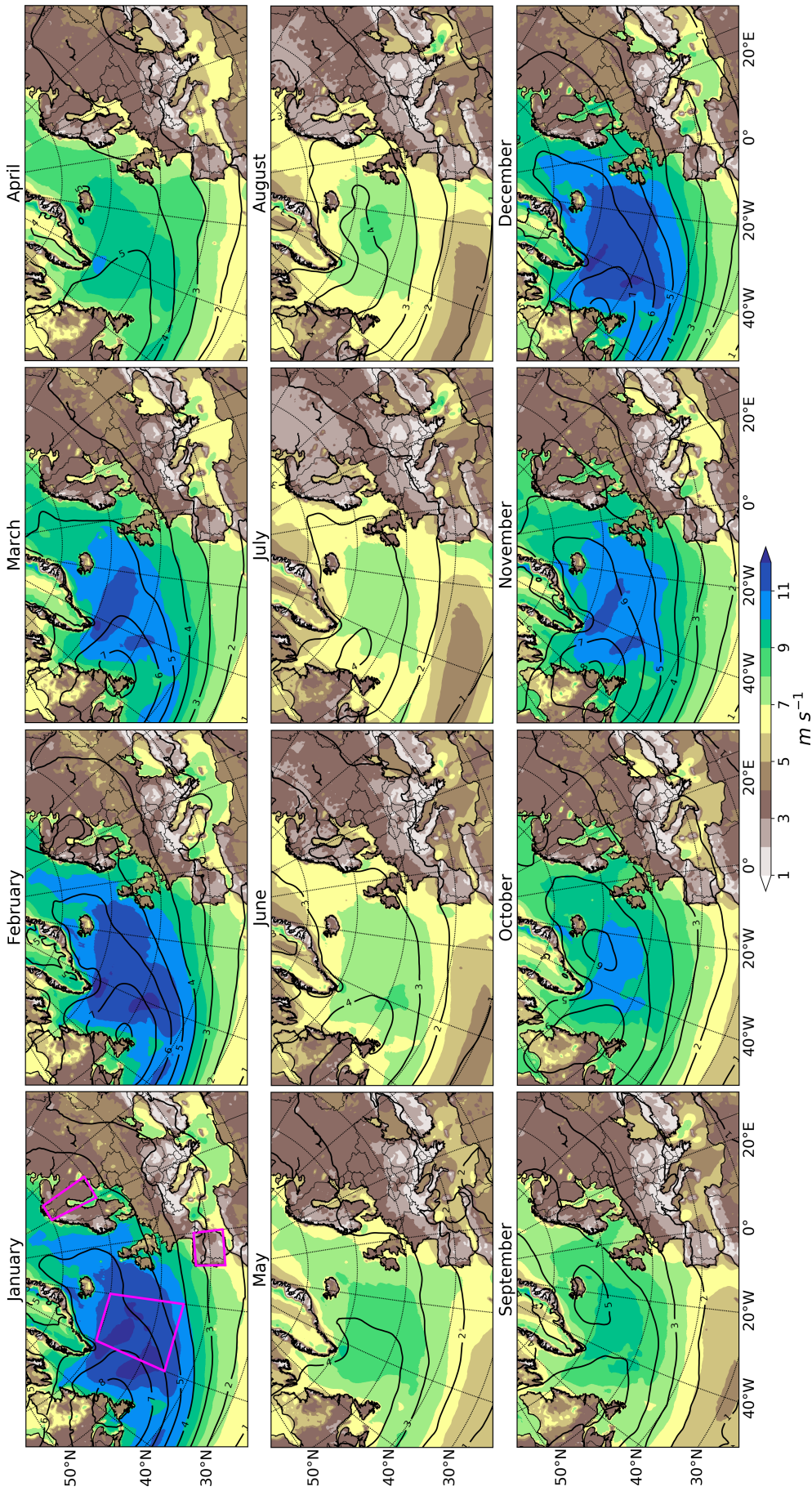


FIGURE 1 Monthly mean values of 10-m wind speed (colours, $m \cdot s^{-1}$) and standard deviation of 2–6 day bandpass filtered mean sea level pressure (contours, hPa) from 1979 to 2018. The magenta boxes shown in the January map are used in time series and trend analysis

Europe most distinctly from October to March. This region is on the southern edge of the storm track (contours in Figure 1) and hence the winds are likely associated with the cyclone activity. The lowest wind speeds over land are found in the high topography regions in the European Alps, Apennines, Pyrenees and Scandinavian Mountains. A similar result is seen in wind climatologies with other reanalyses, for example in NOAA-20CR (Bett *et al.*, 2013) and ERA-40 (Kiss and János, 2008). The IFS is known to have too low wind speeds in complex topography areas in Europe (Hewson, 2020) and for example in Norway, the 10-m winds are underestimated at mountainous stations whereas at coastal stations the observations are quite close to the modelled 10-m wind speeds (Thyness *et al.*, 2017). Similarly in Sweden, monthly wind speeds from ERA5 are underestimated in mountain stations by up to $3.5 \text{ m}\cdot\text{s}^{-1}$ (Minola *et al.*, 2020). This issue may be related to the coarse spatial resolution of the reanalysis or how surface roughness is treated in the IFS. In addition, previous studies (Howard and Clark, 2007; Sandu *et al.*, 2017) have shown that the orographic drag scheme in numerical models give unrealistically low near-surface wind speeds at high altitudes. In contrast to the low wind speeds over European mountainous regions, the high altitudes in Greenland have high wind speeds. A possible explanation might be that the European mountains have more variability in topography at smaller spatial scales than Greenland does (i.e., more subgrid variability). However, it is out with the scope of this current study to rigorously evaluate the accuracy of ERA5 winds in mountainous areas or to determine causes for the apparently underestimate of the 10-m wind speeds in these regions.

In the monthly mean winds, smaller scale wind features are also visible. In all months there is a localized wind speed maximum in the northern Mediterranean Sea. This is the mistral wind phenomenon that blows from the Rhone Valley towards the Gulf of Lion (Zecchetto and De Biasio, 2007). Another local wind speed maximum is present in the eastern Mediterranean Sea, and is especially evident during summer, when this etesians wind feature is the strongest (Zecchetto and De Biasio, 2007). At the southern tip of Greenland, there is a small wind speed maximum visible during most months but this is most pronounced from February to June. This is most likely associated with tip jets and reverse tip jets which are low-level wind speed maxima occurring when a synoptic-scale cyclone interacts with the high topography of southern Greenland (Moore and Renfrew, 2005). In addition, the southeast Greenland barrier winds are seen as a narrow region of high wind speeds between Greenland and Iceland in Denmark Strait from October to February. This agrees with Sampe and Xie (2007) who

found that in winter this region is one of the windiest places in the world's oceans while in summer the occurrence of high wind events is low.

The 98th percentile wind speed over 40-year period (Figure 2) shows similar patterns as the mean wind speed (Figure 1) with a contrast between land and sea areas and a clear seasonal variation. In the North Atlantic storm track region (contours in Figure 1), the highest 98th percentile winds occur between December and March with wind speeds of $20\text{--}22 \text{ m}\cdot\text{s}^{-1}$. The highest 98th percentile winds over land are found during winter in the southern part of Greenland (exceeding $22 \text{ m}\cdot\text{s}^{-1}$) and in Iceland ($14\text{--}16 \text{ m}\cdot\text{s}^{-1}$). The United Kingdom also has high 98th percentile winds during winter ($10\text{--}12 \text{ m}\cdot\text{s}^{-1}$). Over continental Europe, the edge of the storm track region is even more noticeable in the 98th percentile winds than in the mean field.

The same local wind features are found with the 98th percentile wind speeds as with the mean. The highest 98th percentile winds of the mistral wind in the Mediterranean Sea are $18\text{--}20 \text{ m}\cdot\text{s}^{-1}$ during winter months while the etesians are more visible during summer with $12\text{--}14 \text{ m}\cdot\text{s}^{-1}$ winds. Tip jets at the south of Greenland as well as the barrier winds in Denmark Strait are evident through all months. The barrier winds are divided into two to three local wind speed maxima that can be seen from the 98th percentile winds while mean wind field did not capture those details. Similarly, these local wind maxima along the southeast coast of Greenland were found by Moore and Renfrew (2005) using SeaWinds scatterometer and Tuononen *et al.* (2015) using Arctic system reanalysis. It is noteworthy that in addition to the mistral, the etesians, tip jets and barrier winds, there are other local wind phenomena in Europe that are not captured by ERA5. For example, the bora winds that occur most commonly during winter in the Adriatic Sea as a downslope wind phenomenon (Zecchetto and Cappa, 2001) are not seen in the monthly wind climate in ERA5.

Over the 40-year period, the smallest EWF values (below 1.8) occur in the North Atlantic storm track region between November and March and over the low wind speed area at the horse latitudes from May to August (Figure 3). This means that the 98th percentile wind speeds in these regions are not that extreme relative to the mean, i.e. the wind speed distribution is narrow. This implies that during winter the storm track region has constantly high wind speeds while during summer at the horse latitudes there are low winds most of the time. However, at the northern border of the horse latitudes between $20\text{--}40^\circ\text{W}$ and $30\text{--}40^\circ\text{N}$, there is an area with high EWF values up to 2.4 most distinctly visible from June to September. By comparing Figures 1 and 2, we

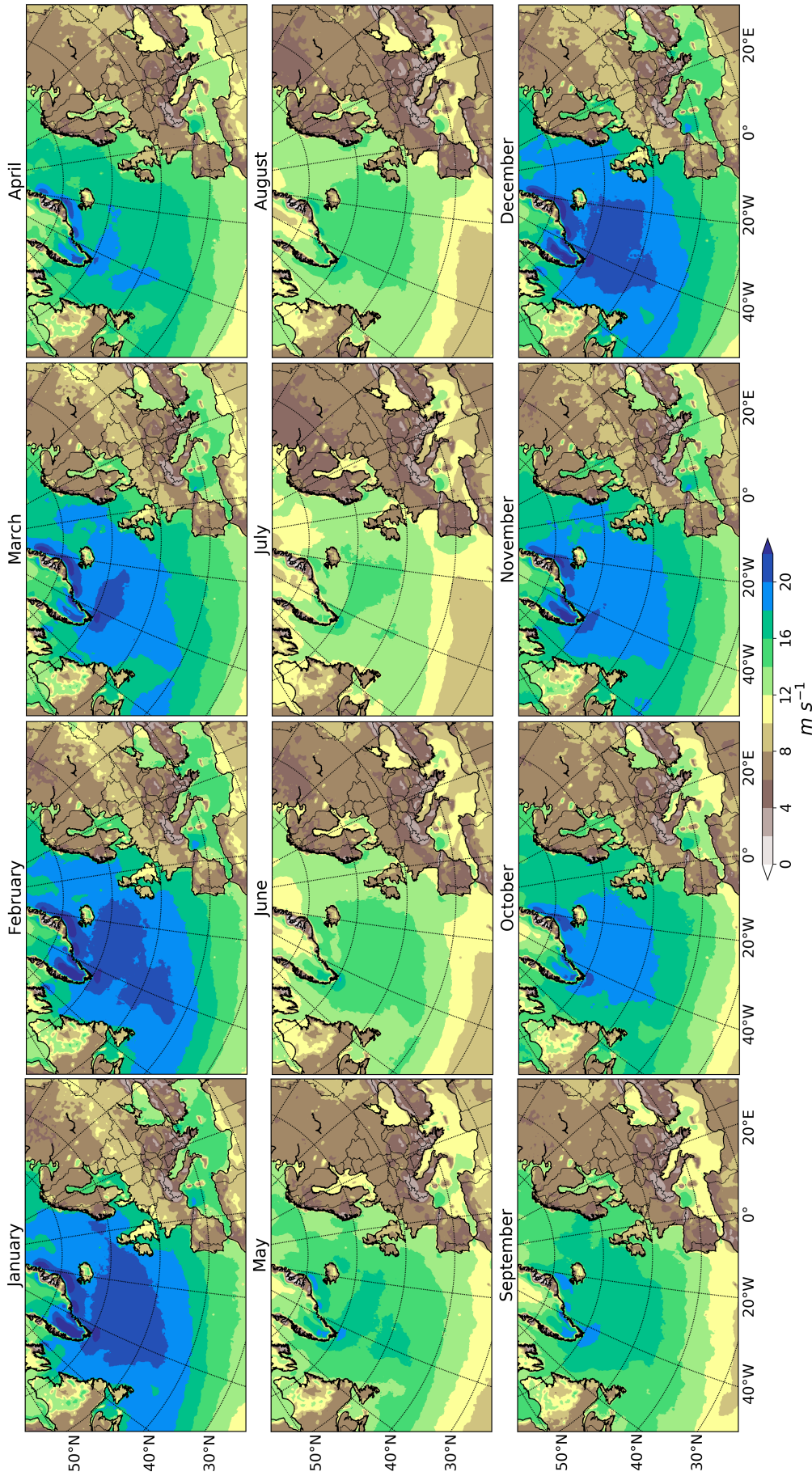


FIGURE 2 Monthly mean values of the 98th percentile of the 10-m wind speed from 1979 to 2018

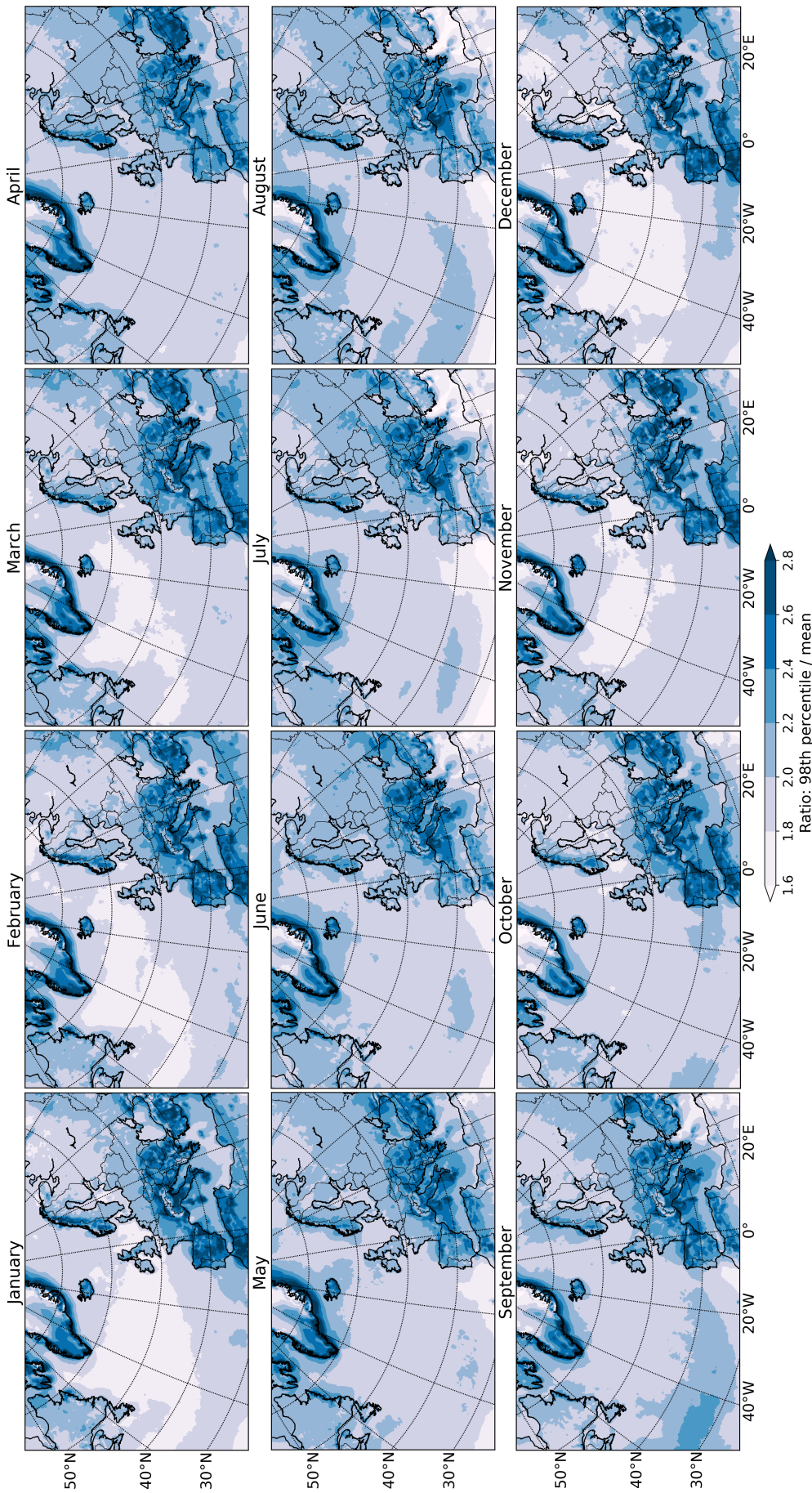


FIGURE 3 Monthly mean values of the 10-m extreme wind factor (EWF) from 1979 to 2018

can see that during those months the border of the low winds does not reach same latitude in the mean and 98th percentile wind speeds. Therefore, while the 98th percentile winds in that region are already getting stronger towards autumn, the mean wind stays relatively low.

Over land, the spatial difference in the EWF values and their seasonality is large (Figure 3). In southern Greenland, Iceland, as well as parts of southern and southeastern Europe such as Italy and Greece, the EWF largely exceeds 2.6 in all months. This implies that the high winds occurring in these regions are very extreme. In Spain and Portugal, the EWF is also as high from September to March but the value drops to 1.8–2.2 during summer. In western Europe, in the United Kingdom and France, the EWF has lower values than in southern Europe but the seasonal variation is similar with higher EWF (up to 2.4) during autumn and winter and lower EWF (down to 1.8) during summer. In contrast, in northern and northeastern Europe, the seasonal variability is the opposite and the EWF difference between seasons is much smaller. For example in Finland, the lowest EWF values of 1.8–2.0 are found from September to March and the highest EWF values of 2.0–2.2 occur during summer. These results indicate that high wind speeds are more common in northern than southern Europe, especially during winter, and therefore the high winds in south are very extreme when they occur. Moreover, it is apparent that the mountains in Norway have very high EWF while the Alps have lower EWF than the surrounding areas. However, as discussed before, we assume that the 10-m winds in mountainous areas in Europe are probably not well represented in ERA5.

To investigate the climatological variability of the 10-m wind speed, Figure 4 shows the standard deviation over the 40-year period. The highest variabilities are found in southern Greenland and its surroundings and over the North Atlantic. These regions were also identified from the mean (Figure 1) and the 98th percentile (Figure 2) wind speeds and they are likely associated with the tip jets, barrier winds and storm tracks. The mistral and the etesians are also evident in the Mediterranean Sea with high values of the standard deviation. This implies that when these phenomena occur the winds are very extreme but otherwise the winds are much calmer.

In addition to the other notable high variability regions, there is also a small, local area in the southwestern coast of Norway which is the most visible during autumn and winter (Figure 4). This location is on the edge of the most frequent storm track region (contours in Figure 1) as well as on the land-sea border. Hence, this area probably has a high wind speed variability due to the storm track shifting: when the storm track is shifted polewards, the winds in this region are extremely high.

The southern edge of the storm track region extending through the central Europe is visible in the standard deviation (Figure 4), as well as in the mean (Figure 1) and the 98th percentile (Figure 2) wind speeds, with the highest variability during winter months.

The monthly distributions of 10-m wind speeds at three locations (the central North Atlantic, Finland and Iberian Peninsula) are given in Figure 5. As was evident from the maps, the temporal variation also shows the seasonal variability with the highest winds during winter and the lowest in summer. Comparing all three locations, the central North Atlantic has the highest variability and the highest absolute wind speeds. A significant difference between these locations is in the EWF seasonality: while the central North Atlantic and Finland have the highest EWF during summer, Iberian Peninsula has its EWF peak during winter. In addition, the variation and absolute values of EWF in Iberian Peninsula are much larger than in the other two regions. This indicates that high wind events in summertime in the central North Atlantic and Finland are rare and therefore if they do occur they are relatively extreme. In contrast, the high winds during wintertime in Iberian Peninsula are very extreme compared to the otherwise relatively low mean winds.

4 | WIND SPEED VARIABILITY AND TRENDS

4.1 | Decadal variability in mean winds

Of all months, February has the largest decade-to-decade variability in the 10-m mean wind speed, closely followed by January and March (Figures 6 and S1). Summer months have the weakest anomalies and thus the smallest variability between the four decades (Figure S2). None of the months show a clear decreasing or increasing trend at any location throughout the 40-year time period but there are variations between the different decades at many locations. In each individual decade, January and February have similar spatial patterns in the 10-m wind speed anomaly (Figure 6). In northern Europe in winter (mainly January and February), the mean wind speeds were relatively weak in the 1980s and 2010s whereas the 1990s was the decade of the strongest winds. The decadal changes are the opposite in southern Europe; the 1980s and 2010s had stronger winds while in the 1990s the winds were weaker. In the 1980s, the northern and eastern part of the North Atlantic had weaker winds whereas in the southern part the winds were stronger. The same but opposite dipole pattern occurred in the 1990s with stronger winds in the northern and eastern parts and weaker winds in the southern part of the North

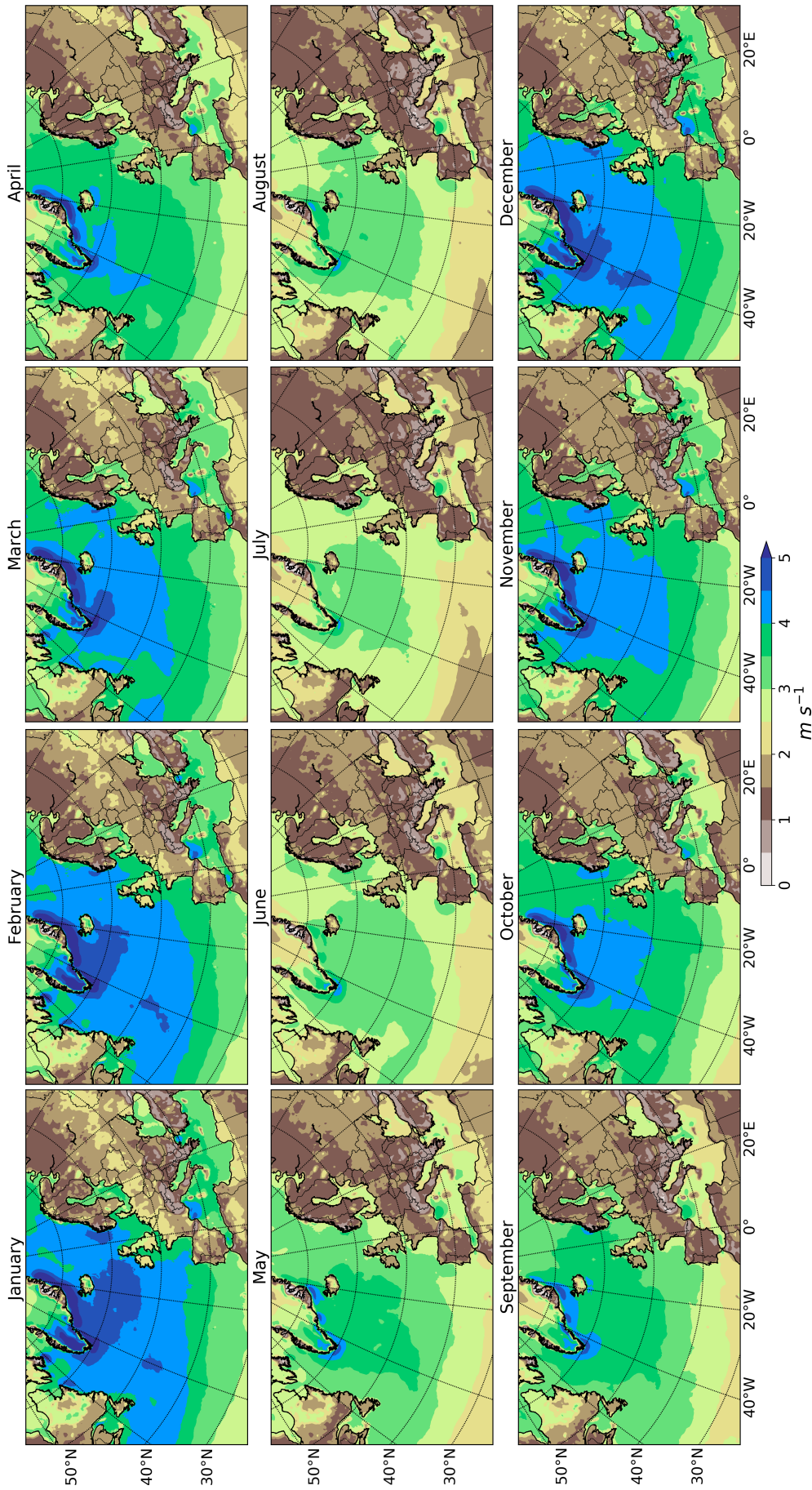
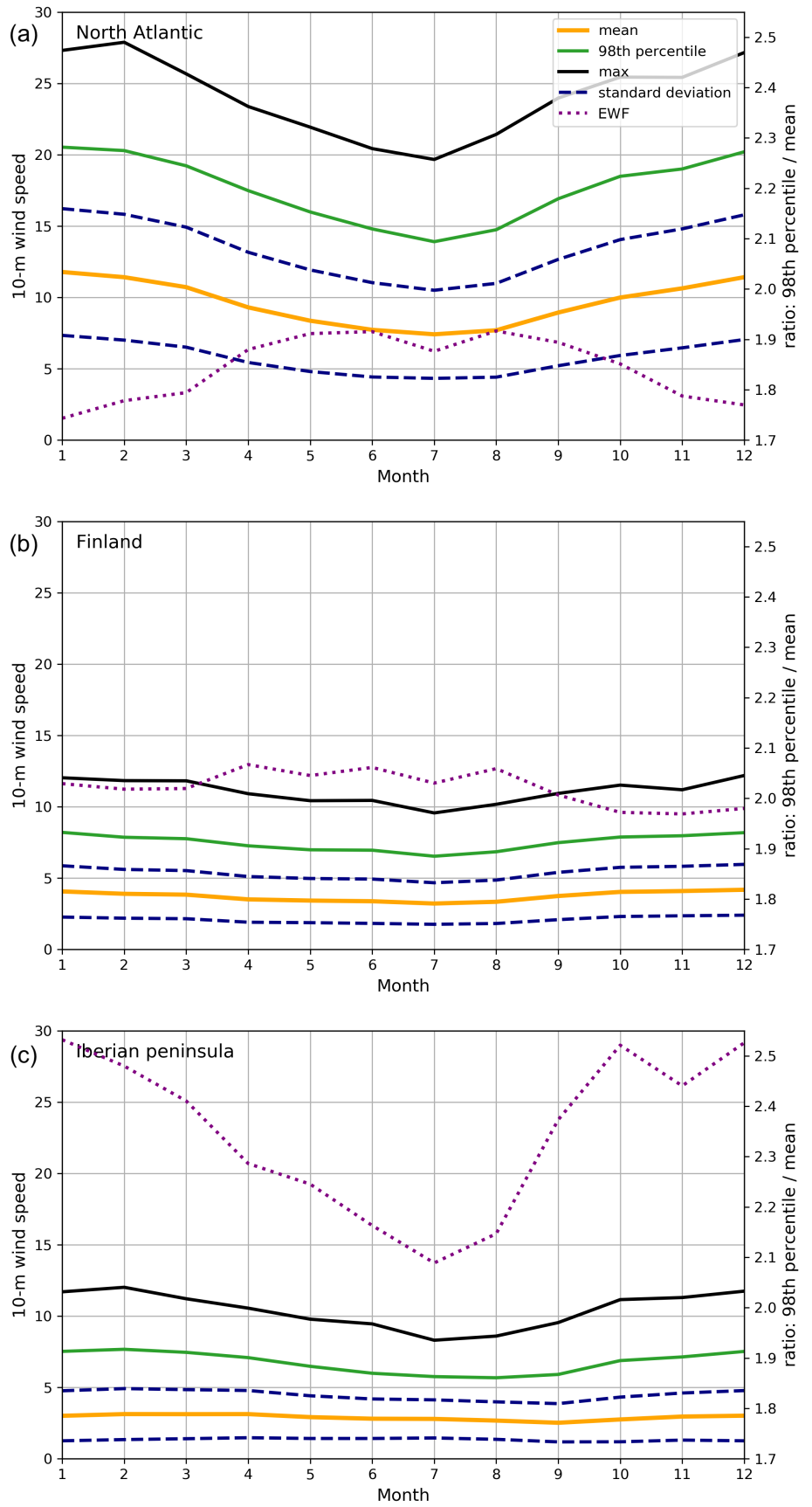


FIGURE 4 Monthly mean values of the standard deviations of 10-m wind speed from 1979 to 2018

FIGURE 5 Monthly mean (orange), 98th percentile (green), maximum (black), ± 1 standard deviation (dashed navy), and extreme wind factor (EWF, dotted purple) of 10-m wind speeds from 1979 to 2018 over (a) the North Atlantic, (b) Finland, and (c) Iberian Peninsula (the boxes are shown in Figure 1)



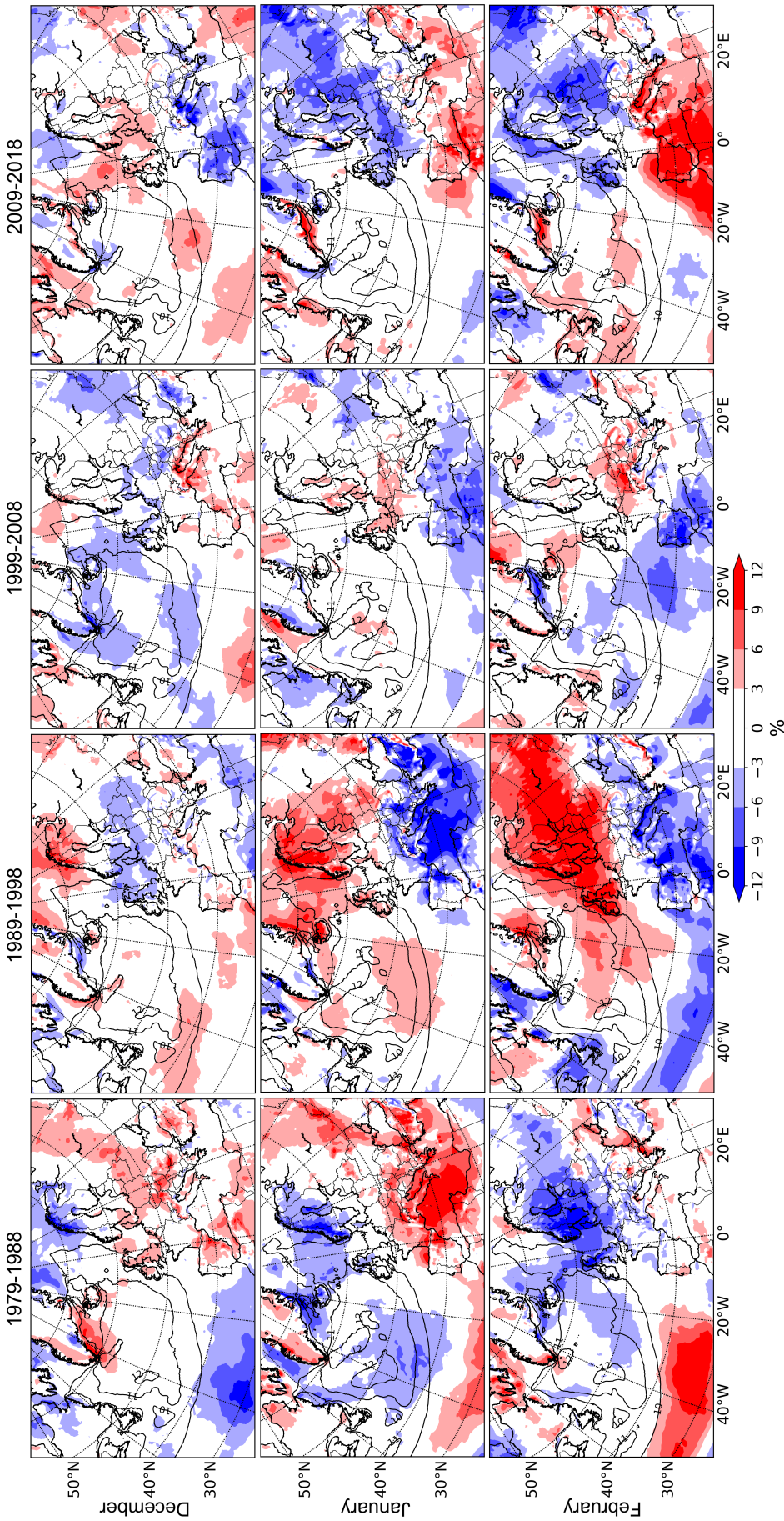


FIGURE 6 Anomalies of the mean 10-m wind speed (colours, m s^{-1}) for December (top row), January (middle row), and February (bottom row) for 10-year periods: 1979–1988 (first column), 1989–1998 (second column), 1999–2008 (third column), and 2009–2018 (fourth column). Contours show the 40-year (1979–2018) means starting at 10 m s^{-1} (same data as shown by the shading in Figure 1)

Atlantic. The physical reasons behind these decadal variations are investigated in Section 5.

In autumn, the mean 10-m winds in the 1980s were stronger than the 40-year climatological mean in northern Europe and weaker, mainly in September, in southern Europe (Figure 7). In the 1990s, September and October were characterized by stronger than average winds in central and southern Europe while in November, northern Europe had weaker winds. The 2010s were mostly less windy than average in all of Europe. The decadal wind variability in the North Atlantic had a dipole pattern in the 1980s with a positive anomaly in the northern parts and a negative anomaly in the southern parts during September and October. In the North Atlantic, the 1990s mainly had weaker winds than the 40-year average whereas the 2010s had stronger winds. In the 2000s in November, there was a tripole pattern with positive anomalies (i.e., stronger winds) in the southwestern and northeastern parts of the North Atlantic and a negative anomaly (weaker winds) in the central part.

4.2 | Decadal variability in EWF

Overall, the signs and spatial patterns of the 98th percentile wind anomalies (not shown) are similar to the mean winds (Figures 6, 7, S1 and S2) even though the 98th percentile fields are more noisy. However, there are some differences in the decadal variability patterns in the EWF (Figures 8, 9, S3, and S4) compared to the mean and the 98th percentile. Since the decadal EWF is calculated by dividing the 10-year 98th percentile by the 40-year mean, a higher EWF in a certain decade indicates that the 98th percentile winds were more extreme relative to the climatological mean and hence possibly more damaging.

By comparing winter months in difference decades, it is apparent that in northern Europe the EWF was the highest in the 1990s (Figure 8) which is also evident in the monthly distribution of the 98th percentile winds and EWF in Finland (Figure 10c and 10d). This further emphasizes that 1990s winter was extremely stormy in northern Europe. In contrast, the lowest decadal EWF in northern Europe was in February in the 1980s and 2010s. Similarly, January and February in central Europe in the 1990s show high EWF i.e. extreme storminess whereas 1980s and 2010s have low EWF. However, in southwestern Europe, the highest EWF is found in January and February in the 2010s which indicates that the winter-time windstorms in the 2010s were more extreme relative to the 40-year climate (Figures 10e and 10f). In the North Atlantic, the most extreme winds occurred in the border of the horse latitudes in February in the 1980s and in

December in the 1990s. A key finding, however, is that the decadal EWF variability in the central North Atlantic is rather small compared to the variations over Europe (Figure 10).

In autumn in northern Europe, winds were the most extreme in October and November in the 1980s and in November in the 2000s whereas the lowest EWF occurred in November in the 1990s and in October in the 2000s (Figures 9 and 10c and 10d). In contrast, in southern Europe, September in the 1990s and October in the 2000s stand out as the most extreme storm months in autumn (Figures 9 and 10e and 10f). Over the North Atlantic, there is more EWF variation in the autumn months than in winter with September having the largest variability (Figure 9). The most extreme storms occurred at the horse latitudes in September in the 2010s. Notable in October is that there is a dipole pattern of lower EWF in the central and higher EWF in the southern part of the North Atlantic in the 1990s and 2010s (Figure 9) which is not apparent in the climatological EWF (Figure 3).

4.3 | Temporal trends

The absolute anomalies of the annual (January–December) mean wind speeds with respect to the 40-year mean in the central North Atlantic, Finland, and Iberian Peninsula are presented as time series in Figure 11. As was estimated from the decadal anomaly maps, there are no clear linear trends over the whole 40-year period and the year-to-year variation is large but some longer term variability is visible. In the central North Atlantic (Figure 11a), the 5-year running means of the mean and the 98th percentile winds show a windier period between 1990 and 1995. After 1995 the wind speeds decreased until 2010 after which there has been an increase until 2018. The magnitudes as well as the time evolution of the anomalies for the 98th percentile wind speed in the central North Atlantic are similar to the anomalies in the mean wind speed. Similar annual variability was found in the northeast Atlantic storminess which was analysed from the 95th and 99th percentiles of geostrophic wind speeds calculated from surface pressure observations (Krueger *et al.*, 2019). Krueger *et al.* (2019) found a maximum wind speed peak between 1990–1995 and a minimum peak around 2010 which corresponds well to our results from ERA5 in the central North Atlantic (Figure 11a).

In Finland (Figure 11b), there is a bigger difference between the mean and the 98th percentile with the latter having larger variability although the time evolutions are alike. There was a peak of stronger winds around 1990–1995, as was found in the central North Atlantic.

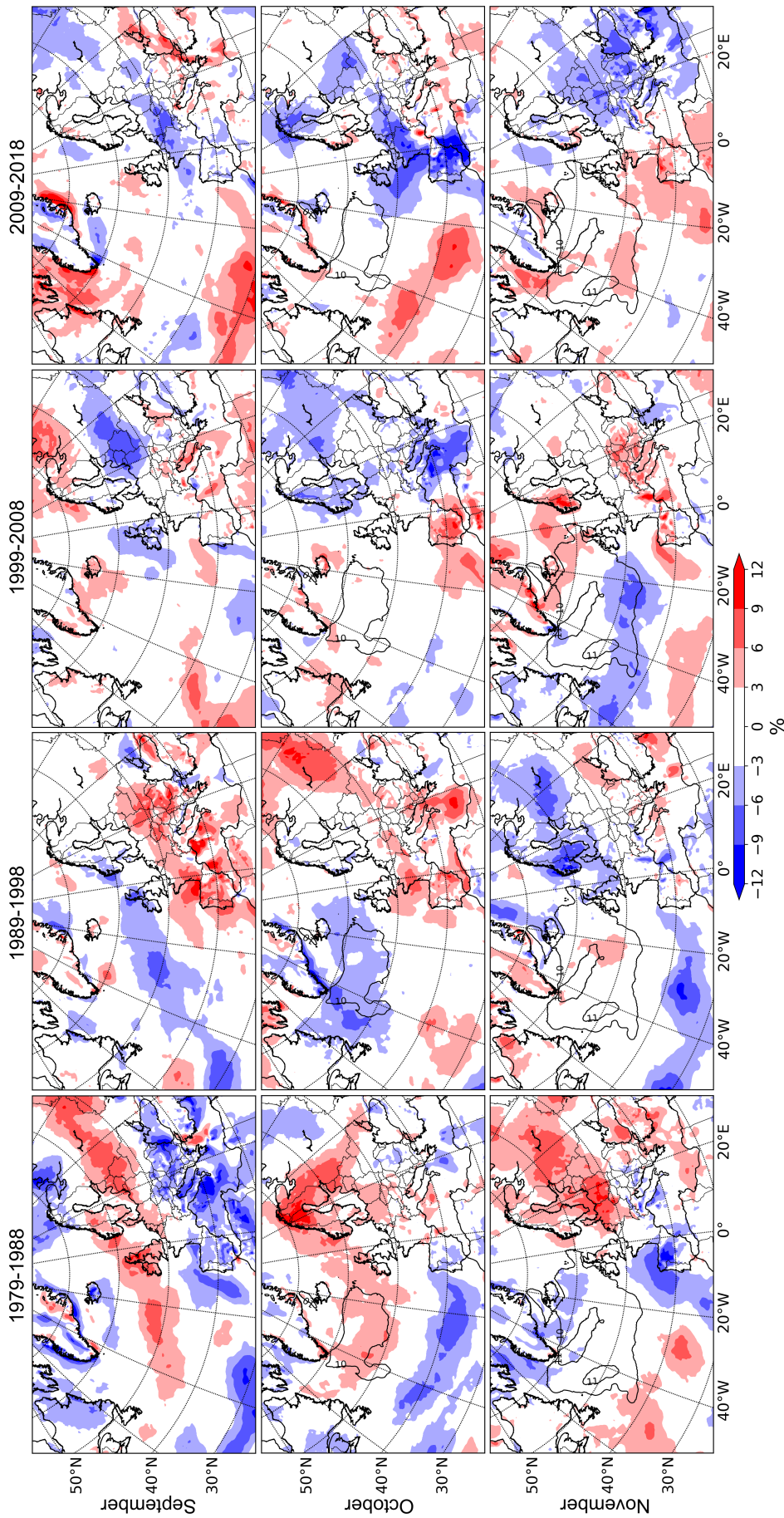


FIGURE 7 Anomalies of the mean 10-m wind speed (colours, $\text{m}\cdot\text{s}^{-1}$) for September (top row), October (middle row) and November (bottom row) for 10-year periods: 1979–1988 (first column), 1989–1998 (second column), 1999–2008 (third column), and 2009–2018 (fourth column). Contours show the 40-year (1979–2018) means starting at $10 \text{ m}\cdot\text{s}^{-1}$ (same data as shown by the shading in Figure 1)

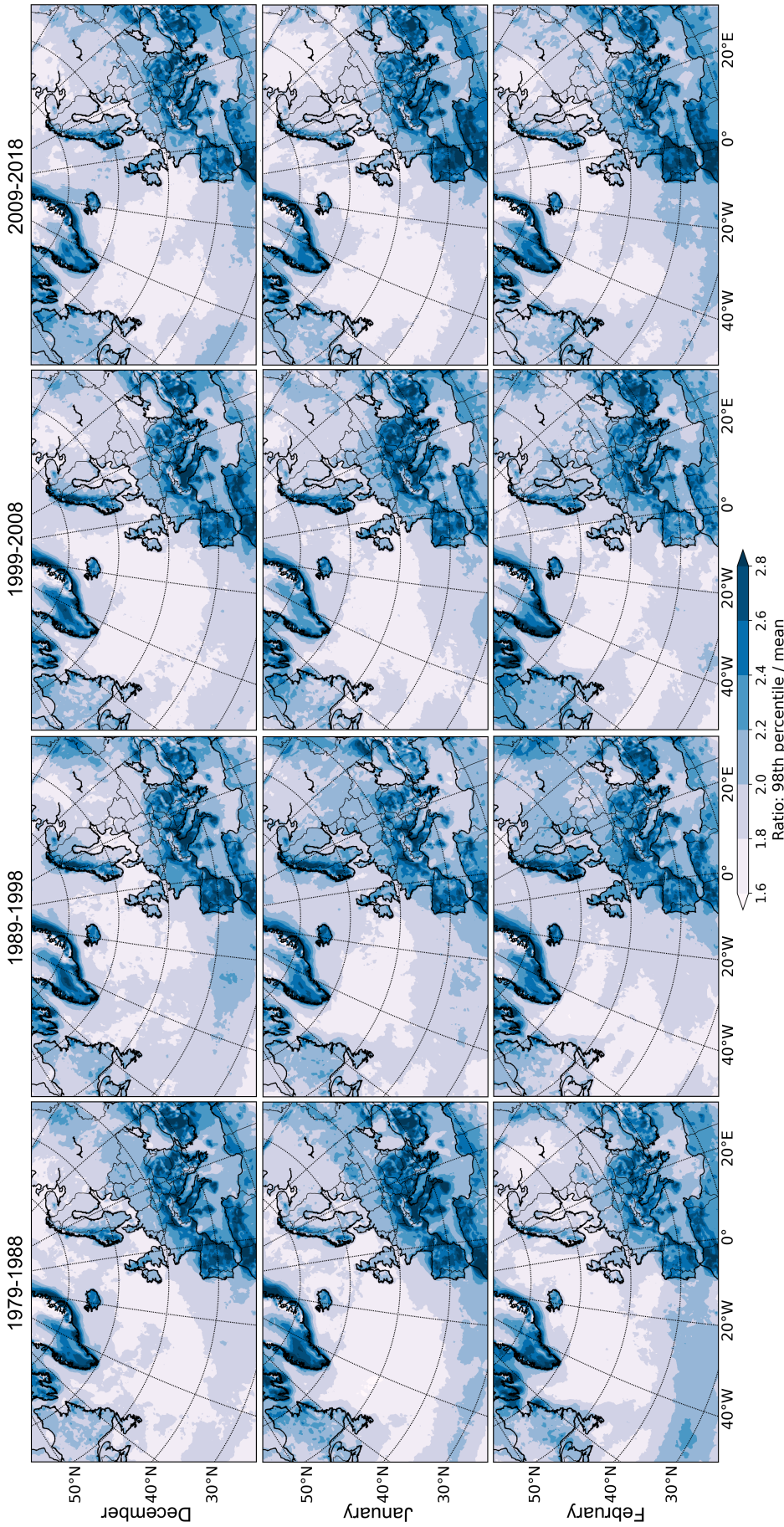


FIGURE 8 10-m extreme wind factor (EWF) (colours, m s^{-1}) for December (top row), January (middle row) and February (bottom row) for 10-year periods: 1979–1988 (first column), 1989–1988 (second column), 1999–2008 (third column), and 2009–2018 (fourth column)

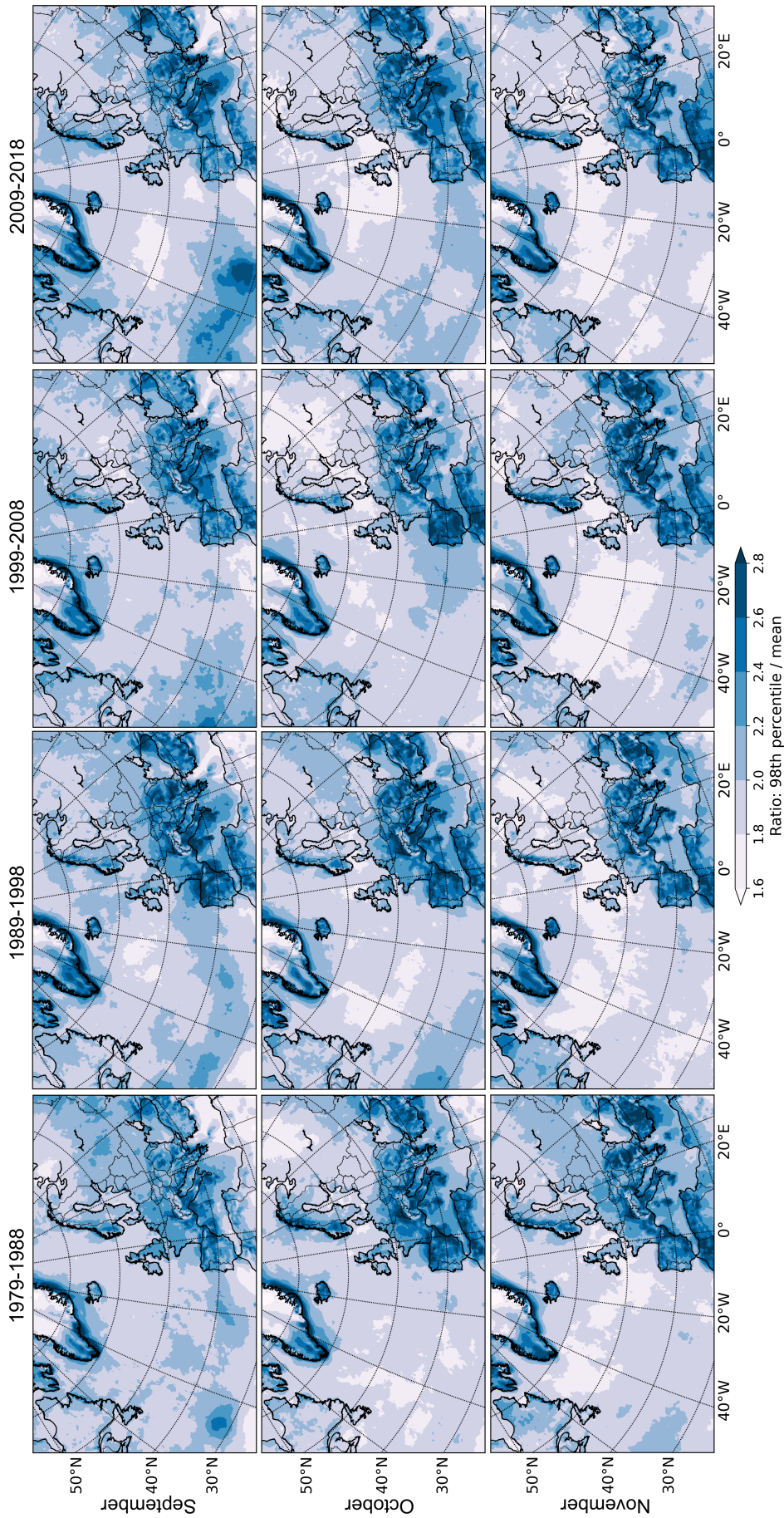


FIGURE 9 10-m extreme wind factor (EWF) (colours, $\text{m}\cdot\text{s}^{-1}$) for September (top row), October (middle row), and November (bottom row) for 10-year periods: 1979–1988 (first column), 1989–1988 (second column), 1999–2008 (third column), and 2009–2018 (fourth column)

From there forward, there has been a decreasing trend in wind speeds for many decades until around 2014 when a transition to a period with no trends has taken place. The annual mean wind speed variations are similar as in Laapas and Venäläinen, (2017) who used mean and maximum wind speed observations in Finland in 1959–2015 and found positive wind speed anomalies until 1995 and negative anomalies until around 2014. Likewise in our results from ERA5, Laapas and Venäläinen (2017) found the strongest positive annual anomalies during period 1979–2015 in 1992, 1995, and 2015 and a negative anomaly peak in 2002.

In Iberian Peninsula (Figure 11c), the 5-year running mean of mean winds shows an increasing trend from 1980 to 2000, a decrease until 2006 and again an increase until 2014. The variability is larger in the 98th percentile winds with the most evident negative anomaly, i.e. weaker winds, between 2003 and 2007. Comparing our results from ERA5 to wind speed observations from land stations studied separately for Spain and Portugal in 1961–2011 by Azorin-Molina *et al.* (2014), similar annual variability is seen, for example the negative anomalies in 1997, 1998 and 2011 and positive anomalies in 1979, 1996, and 2001. However, when considering the longer

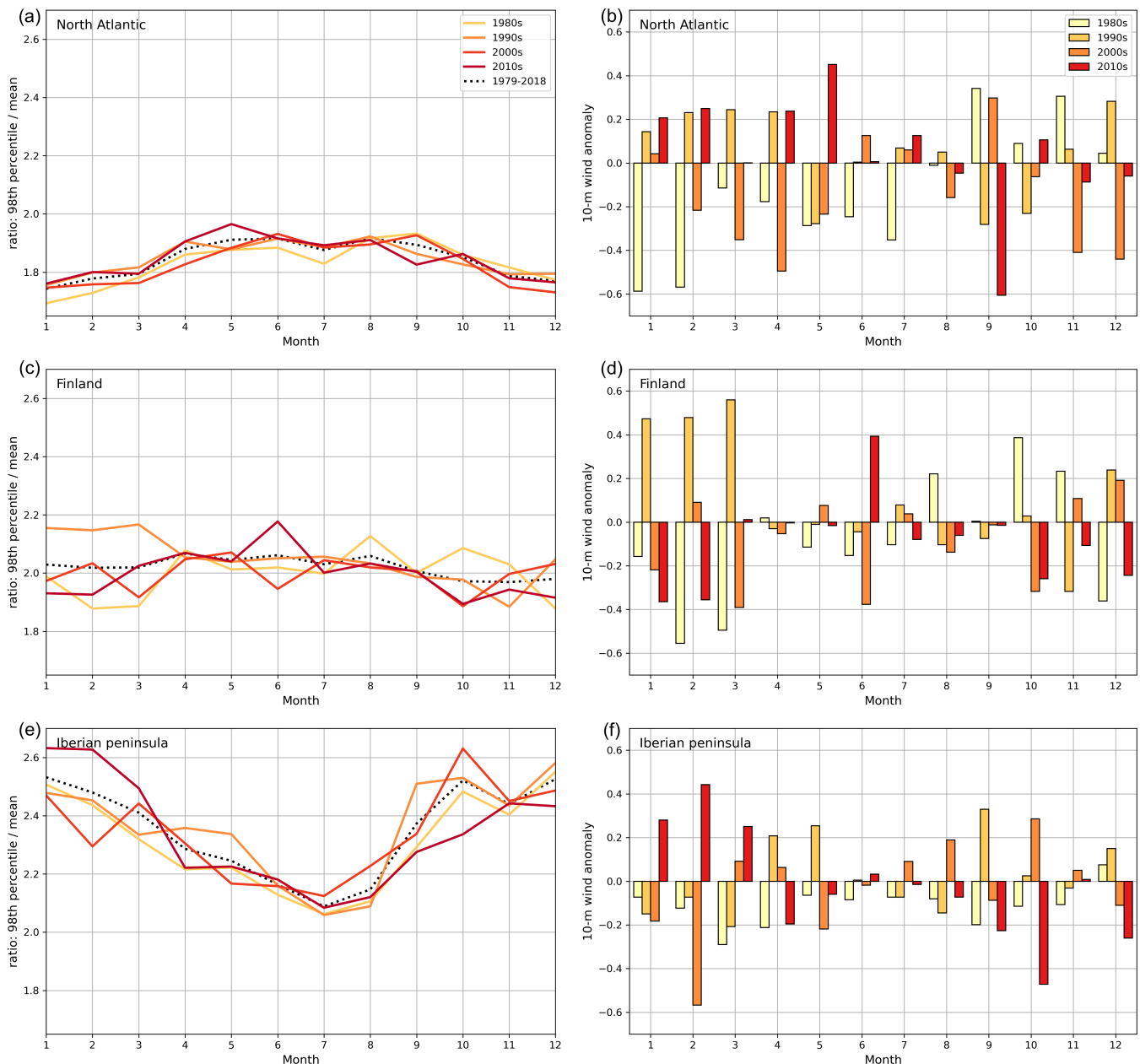


FIGURE 10 Left panel: Monthly extreme wind factor (EWF) for 10-year periods, and right panel: Monthly mean anomalies (10-year value minus 1979–2018 mean value) of the 98th percentile wind speed. Panels (a) and (b) show the North Atlantic; (c) and (d) Finland; and (e) and (f) Iberian Peninsula (location boxes are shown in Figure 1)

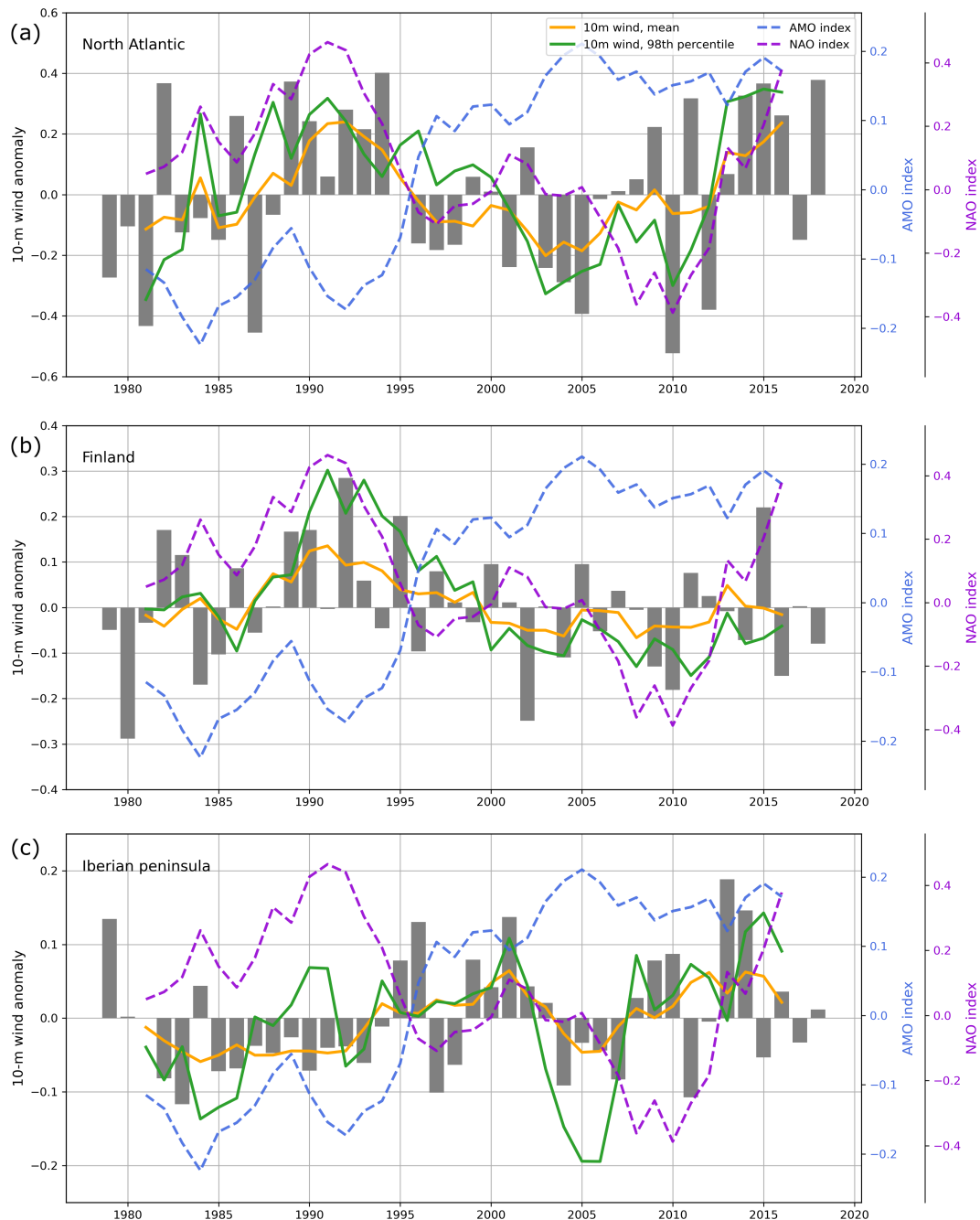


FIGURE 11 Annual 10-m wind speed anomalies (yearly mean value minus the 1979–2018 mean value, grey bars), 5-year running mean of the mean (orange) and 98th percentile (green) 10-m wind speeds, and the AMO (dashed navy) and NAO (dashed purple) indices (also 5-year running means) over (a) the North Atlantic, (b) Finland, and (c) Iberian Peninsula (the boxes are shown in Figure 1). Note that the y-axes have different scales

term trends, Azorin-Molina *et al.* (2014) found the period of 1980–2000 to have a declining trend contradictory to our results from ERA5 and the increasing trend from Azorin-Molina *et al.* (2014) starts around 1998, i.e. 8 years earlier than in our analysis. Azorin-Molina *et al.* (2014) used a 15-year Gaussian low-pass filter and anomalies relative to period 1981–2010 while we used a 5-year running mean relative to 1979–2018 which may

explain some differences in the long-term trends in addition to, e.g. surface roughness which has influences in station-based analysis (Vautard *et al.*, 2010; Azorin-Molina *et al.*, 2014).

The smallest annual variation in wind speeds in these three locations is found in Iberian Peninsula (Figure 11) which is consistent with the fact that it has the lowest wind speeds overall (Figure 5). However, to better compare these

regions we should consider relative anomalies. In relative terms (not shown), the annual anomalies in Figure 11 are largest over Finland (-7.6% to 7.5%) and smallest in the North Atlantic (-5.5% to 4.2%). In Iberian Peninsula, the relative anomalies range from -4.0% to 6.5% .

The wind speed time series revealed some periods with increasing trends and other periods with decreasing trends in all locations (Figure 11). Table 1 shows the annual and monthly linear trends for the whole 40-year time period. The calculated annual mean and the 98th percentile wind trends are positive in the central North Atlantic and Iberian Peninsula and negative in Finland. However, the magnitudes of the trends are small and most importantly the trends are not statistically significant at the 5% level in the Mann-Kendall test. The only statistically significant trends are an increase in mean winds in May in the central North Atlantic and in August in Iberian Peninsula. To conclude, there are no linear wind speed trends over the 40-year period, however, our analysis shows there is pronounced variability between different decades.

5 | PHYSICAL REASONS FOR 10-M WIND SPEED VARIABILITY

5.1 | Correlation between monthly 10-m and 300-hPa wind speeds

To examine how the near-surface and upper-level winds are related we calculated monthly correlation between

10-m and 300-hPa wind speeds from 1979 to 2018 (Figure 12). The highest correlation in all months, being the strongest in winter, is found in the exit region of the jet stream over the North Atlantic. The highest correlation over land occurs in the United Kingdom in December and January and in Iberian Peninsula, Germany and Poland in January. The winds correlate in most of Europe from October to March excluding the eastern parts. From June to July, there is a band from western to northern Europe with high correlation. Therefore, in most of the North Atlantic and Europe, especially in wintertime, the 10-m winds are generally well correlated with the upper-level winds and the jet stream. In contrast, the weakly negative correlations in the coastal areas of Greenland through all months (Figure 12) may indicate that its wind phenomena are the result of local processes (i.e., tip jets and barrier winds) rather than the large-scale atmospheric patterns.

5.2 | Decadal variability in 10-m and 300-hPa wind speed, mean sea level pressure, and storm tracks

The correlation between the 10-m and 300-hPa wind speeds is also seen at the decadal scale in February; where the decade has been windier than average similarly the upper-level winds in that location have been stronger and vice versa (Figure 13). The 1980s in February had weaker 10-m winds in northern Europe which was due to a equatorward shift in the jet stream

TABLE 1 Monthly and annual trends ($\text{m}\cdot\text{s}^{-1}\cdot\text{decade}^{-1}$) of the mean and 98th percentile 10-m wind speeds in the North Atlantic, Finland and Iberian Peninsula (the boxes are shown in Figure 1). Values shown in bold are statistically significant at the 5% level

	North Atlantic		Finland		Iberian Peninsula	
	Mean	98th percentile	Mean	98th percentile	Mean	98th percentile
January	0.110	0.259	0.006	-0.092	0.018	0.080
February	0.054	0.117	0.007	-0.029	0.121	0.206
March	0.036	0.024	0.024	0.066	0.051	0.123
April	0.085	0.083	-0.014	-0.032	-0.026	-0.062
May	0.146	0.131	0.031	0.031	-0.014	-0.020
June	0.130	0.096	0.007	0.105	0.030	0.078
July	0.037	0.100	-0.013	-0.045	0.049	0.025
August	-0.033	0.051	-0.028	-0.062	0.037	0.054
September	-0.047	-0.143	0.018	0.009	0.013	-0.013
October	-0.087	0.086	-0.088	-0.135	-0.050	-0.117
November	0.040	-0.112	-0.044	-0.073	0.047	0.020
December	0.007	-0.075	0.018	-0.021	-0.108	-0.147
Annual	0.038	0.098	-0.013	-0.028	0.014	0.034

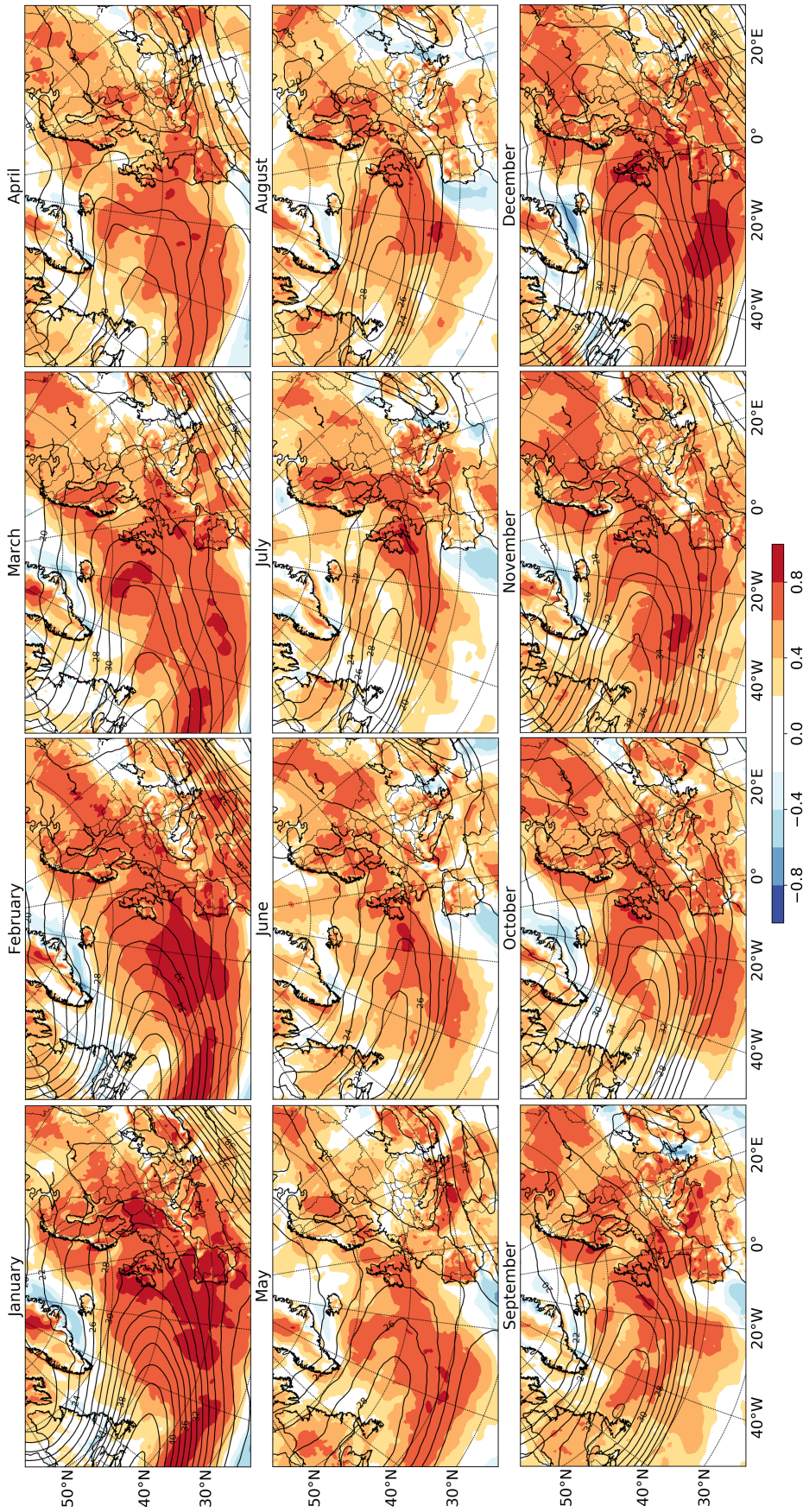


FIGURE 12 Monthly correlation coefficients (shading) between the 10-m and 300-hPa wind speeds from 1979 to 2018. The contours are the monthly mean 300-hPa wind speeds (starting at 20 m·s⁻¹ and with a 2 m·s⁻¹ contour interval)

and storm tracks and a weaker than average pressure gradient (Figure 13). The tripole pattern in the 300-hPa wind anomaly indicates meridional fluctuation in the jet position which together with the anomalously high surface pressure in Scandinavia implies a tendency towards more blocking events (Rex, 1950). The stronger winds in the southern part of the North Atlantic were in the area of stronger upper-level winds. The extremely stormy February in northern Europe in the 1990s was a result of a stronger, poleward and eastward extended jet stream and storm track region and a stronger than average pressure gradient (Figure 13). Accordingly, the winds were

weaker in southern Europe. While in the 1980s and 1990s the dipole anomaly patterns were more north-south oriented, in the 2000s and 2010s the dipole was orientated south-west to north-east. In the 2010s, the polar jet stream was shifted eastward and appears to almost merge with the stronger and northward shifted subtropical jet. In addition, there was a local lower pressure area in southern Europe and higher pressure in northern Europe which potentially indicates an increased tendency of cut-off low and blocking high situations. The storm tracks were shifted south and east. These conditions caused extreme storms in southwestern Europe

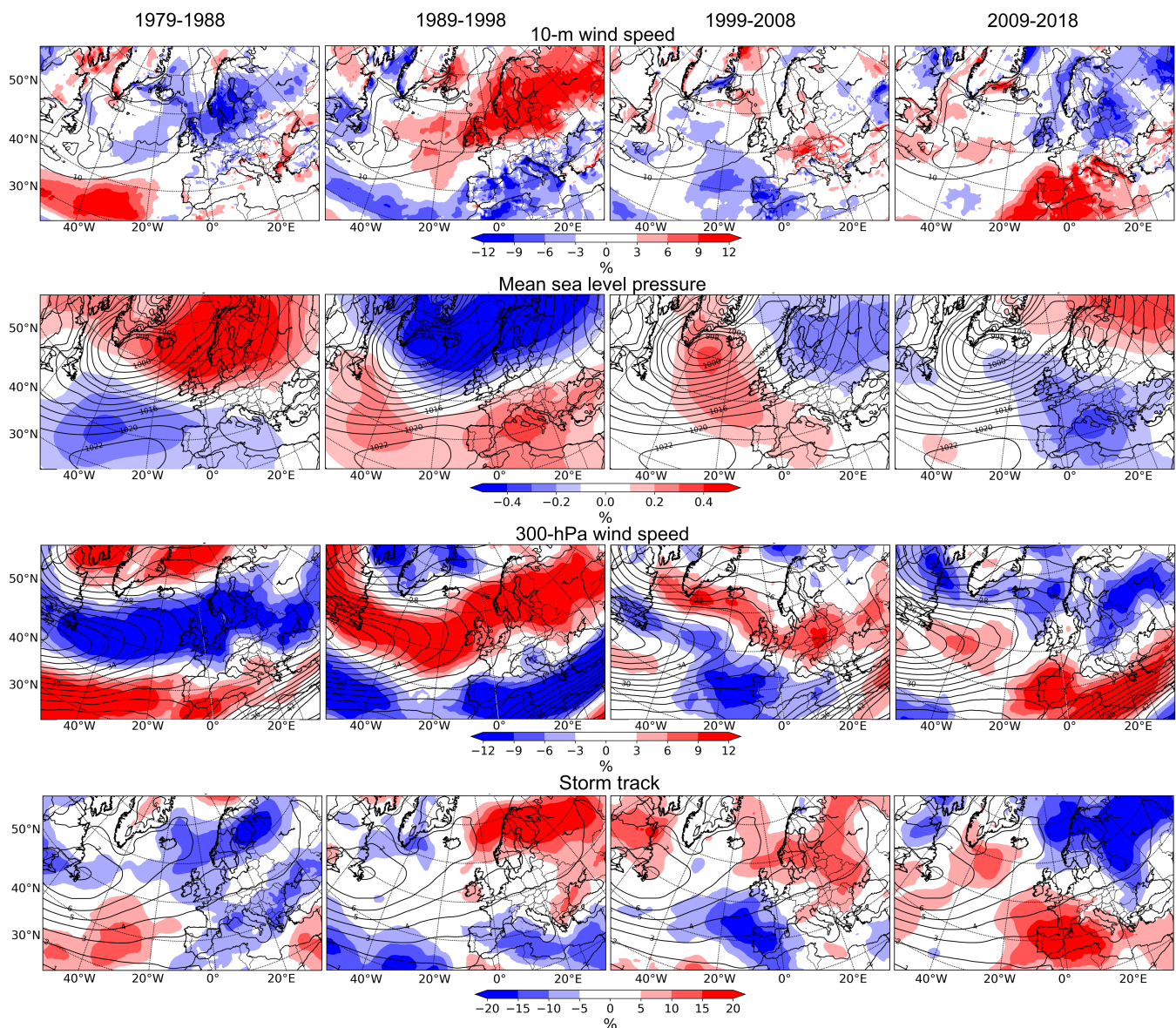


FIGURE 13 Anomalies (colours) and the 40-year means (contours) in February of the mean 10-m wind speed (first row, contours start at 10 m s⁻¹), mean sea level pressure (second row, contours at 1 hPa interval), 300-hPa wind speed (third row, contours at 2 m s⁻¹ interval), and storm tracks as standard deviation of 2–6 day bandpass filtered mean sea level pressure (fourth row, contours at 1 hPa interval) for 10-year periods: 1979–1988 (first column), 1989–1998 (second column), 1999–2008 (third column), and 2009–2018 (fourth column)

while the rest of Europe had calmer winds. We similarly investigated the decadal variability in October and found the same consistency between the 10-m wind anomalies and 300-hPa wind, MSLP and storm track anomalies (not shown).

5.3 | Correlation between temporal variability in 10-m wind speed and the NAO and AMO

When annual mean values are considered in the three locations, the temporal changes in wind speeds follow the NAO index really well in the central North Atlantic (Figure 11a) and Finland (Figure 11b) whereas in Iberian Peninsula (Figure 11c) the correlation is weaker. The annual correlations between the NAO index and the mean and the 98th percentile winds are statistically significant in the central North Atlantic (Figure 14a) and Finland (Figure 14c) but not in Iberian Peninsula (Figure 14e). On monthly scales, the correlation is significant in the central North Atlantic from October to May and in Finland from September to March with higher correlations mostly with the mean winds than the 98th percentile. Although the annual NAO does not correlate with the mean or the 98th percentile winds in Iberian

Peninsula the majority of the months between July and March do have a significant negative correlation, especially with the mean winds. These results are expected since positive NAO is linked to a stronger than average pressure gradient between the northern and southern North Atlantic which leads to more storminess in northern Europe and less in southern Europe (Hurrell, 1995). The linkage between long-term wind speed changes and the NAO was similarly found by Zeng *et al.* (2019) and Azorin-Molina *et al.* (2018).

The annual AMO index in the 40-year time period appears to have a negative correlation with the NAO index (Figure 11). A positive AMO may induce a negative winter NAO by reducing the SST gradient and hence leading to a decrease in the North Atlantic storm track activity (Sutton *et al.*, 2018). However, there is no consensus on how the NAO and AMO are related, and the relationship depends on which dataset and which methods are used (Peings and Magnusdottir, 2014). Our results show that only the annual mean wind speeds in the central North Atlantic have significant negative correlation with the AMO index but the correlation is quite weak (Figure 14b). On the monthly scale, the mean winds in the central North Atlantic are negatively correlated with the AMO in March and November, the 98th percentile winds additionally in April and December. None of the

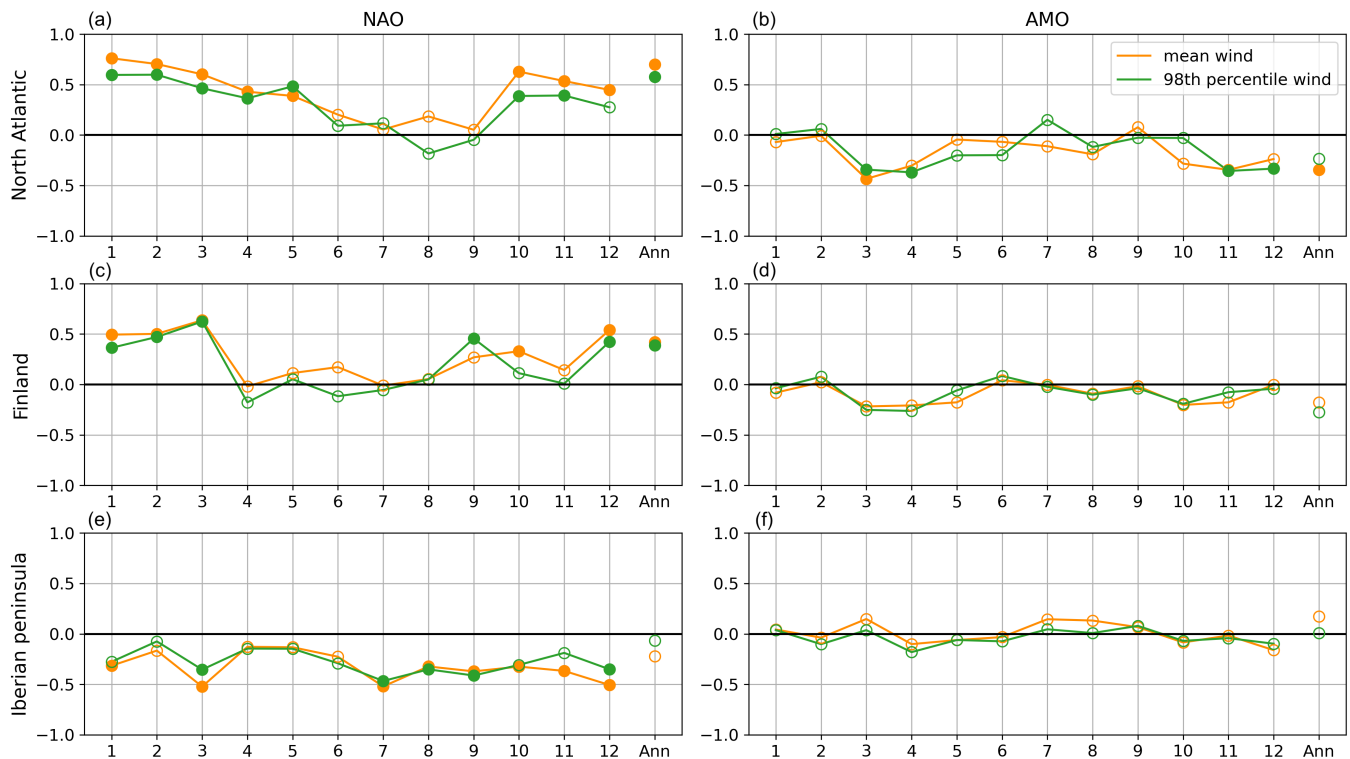


FIGURE 14 Monthly and annual correlation coefficients (circles) between the NAO and AMO indices and the mean (orange) and 98th percentile (green) 10-m wind speeds in (a) and (b) the North Atlantic; (c) and (d) Finland and (e) and (f) Iberian Peninsula (the boxes are shown in Figure 1). Values with filled circles are statistically significant at the 5% level

months nor the annual mean correlate in Finland (Figure 14d) or Iberian Peninsula (Figure 14f). Hence, our results show that while the AMO correlates moderately with the annual wind speeds, as well as few spring and winter months, in the central North Atlantic, there are no correlation in Finland and Iberian Peninsula.

6 | CONCLUSIONS

In this study, we analysed the 10-m wind speed climatology, decadal variability and possible trends in the North Atlantic and Europe in ERA5 reanalysis from 1979 to 2018. Furthermore, we examined the physical reasons for the 10-m wind speed variability. To investigate the extremeness of the wind speeds we defined an extreme wind factor (EWF) which is a ratio of the 98th percentile and mean wind speeds. In addition to spatial and decadal variations in the North Atlantic and Europe domain we studied the temporal changes in wind speeds in three locations: the central North Atlantic, Finland and Iberian Peninsula.

The 10-m wind speed climate in ERA5 shows a distinct land-sea gradient and a seasonal variation with the strongest mean and the 98th percentile winds over the ocean and during winter months. The strongest winds are associated with the storm track region over the ocean in the central North Atlantic and over land in a narrow band across central Europe. The known underestimation of 10-m winds in areas of high topography in numerical models (Howard and Clark, 2007; Hewson, 2020) appears to also be present in ERA5, for example, in the European Alps and Scandinavian Mountains. In the monthly wind climate, ERA5 captures some smaller scale local phenomena: the mistral and the etesians in the Mediterranean Sea and tip jets and barrier winds near Greenland. The largest variability, in terms of the standard deviation, is co-located with the highest wind speeds and hence is also associated with the storm tracks and local wind phenomena.

The EWF is low over the central North Atlantic which indicates a narrow wind speed distribution. In Europe, the magnitude and seasonal variation of EWF differs between areas. In all months, the EWF is higher in southern Europe than in northern Europe implying that the wind speed distribution is broader with a more positively skewed tail in southern Europe compared to northern Europe. In the Iberian Peninsula, the EWF is the highest during winter months whereas in Finland the highest values occur during summer. This implies that in Finland, windstorms are more common in winter and high wind events in summertime are more extreme because of their rare occurrence.

The spatial and decadal 10-m wind speed variability was analysed in four 10-year periods and we found differences between the decades with winter months having the largest decade-to-decade variability. The spatial changes in the mean and the 98th percentile wind speed anomalies are similar, however, the spatial changes in the decadal EWF shows differences compared to those. The 10-m mean wind speed anomalies in northern and southern Europe were mostly the opposite at each decade; the 1980s and 2010s had stronger than average winds in southern Europe whereas the 1990s was extremely stormy in northern Europe. In addition to decadal variation in 10-m wind speeds, annual and monthly trends were calculated at the three locations. Our results show that there are mostly no significant linear wind speed trends in the 40-year time period.

Lastly, we investigated what are the physical reasons for the 10-m wind speed variations by examining the monthly correlation with the 300-hPa winds and the decadal variability in February in comparison to the 300-hPa wind speed, MSLP and storm tracks. In addition, the temporal variability was investigated at the three locations in relation to the NAO and the AMO. The 10-m winds correlate well with the 300-hPa wind speeds in most of the North Atlantic and Europe, particularly in cold season months and in the exit region of the jet stream. The weaker than average 10-m winds in northern Europe in winters of 1980s and 2010s were caused by an equatorward shift of the jet stream and storm tracks and a weaker than average pressure gradient over the North Atlantic. In contrast, the extremely windy decade of 1990s in northern Europe, while winds were weaker in southern Europe, was due to a poleward and eastward shifted jet stream and storm tracks and a stronger than average north-south pressure gradient. Hence, the decadal changes in the 10-m wind speeds in the North Atlantic and Europe can be largely explained by the positioning of the jet stream and storm tracks and the strength of the north-south pressure gradient in the North Atlantic.

The 10-m winds in the central North Atlantic and Finland have an expected significant positive correlation with the NAO index on annual timescales as well as during cold season months. The correlation is negative in the Iberian Peninsula and significant in most months between July and March. Of the three locations, the AMO index has a significant negative correlation only in the central North Atlantic on annual scales and in a few months in spring and winter. Therefore, we find that the AMO does not influence the wind speeds over Finland and Iberian Peninsula.

As our results highlight, the annual and decadal variability in wind speeds is large and hence the

climatological anomalies and trends are highly dependent on the chosen time period (Troccoli *et al.*, 2012). The 10-m wind speed variability is related to the large-scale circulation which exhibits decadal variations. Therefore, although the linear trends can reveal an overall trend in long term, a broader view of the wind speed changes are attained by considering the inter-annual or decadal variability.


Climatological studies, such as the one presented here, do have certain limitations. For example, extreme events such as one powerful storm are not necessarily visible and decreasing trends in wind speed do not exclude possible opposite trends in rare extreme events. Furthermore, this study does not attempt to quantitatively determine what type of weather phenomenon the winds are related to. Many previous studies (e.g., Feser *et al.*, 2015; Gregow *et al.*, 2020) have examined trends and characteristics of extratropical cyclones and the winds related to these systems. However, the comparison of wind speed and windstorm climates is difficult and would be a key next step to improve understanding of their linkages.

ACKNOWLEDGEMENTS

This work was supported by the Finnish Cultural Foundation (Satakunta Regional Fund/ Aili Nurminen Fund, grant no. 75181580), MONITUHO project, the EU through the ERA4CS WINDSURFER project, CLIPS project and the Academy of Finland (grant no. 307331).

ORCID

Terhi K. Laurila  <https://orcid.org/0000-0002-0903-7331>

Victoria A. Sinclair  <https://orcid.org/0000-0002-2125-4726>

Hilppa Gregow  <https://orcid.org/0000-0003-3805-2247>

REFERENCES

- Azorin-Molina, C., Vicente-Serrano, S.M., McVicar, T.R., Jerez, S., Sanchez-Lorenzo, A., López-Moreno, J.-I., Revuelto, J., Trigo, R.M., Lopez-Bustins, J.A. and Espirito-Santo, F. (2014) Homogenization and assessment of observed near-surface wind speed trends over Spain and Portugal, 1961–2011. *Journal of Climate*, 27(10), 3692–3712.
- Azorin-Molina, C., Rehman, S., Guijarro, J.A., McVicar, T.R., Minola, L., Chen, D. and Vicente-Serrano, S.M. (2018) Recent trends in wind speed across Saudi Arabia, 1978–2013: a break in the stilling. *International Journal of Climatology*, 38(S1), e966–e984.
- Bett, P., Thornton, H. and Clark, R. (2017) Using the twentieth century reanalysis to assess climate variability for the European wind industry. *Theoretical and Applied Climatology*, 127, 61–80.
- Bett, P.E., Thornton, H.E. and Clark, R.T. (2013) European wind variability over 140 yr. *Advances in Science and Research*, 10(1), 51–58.
- Blackmon, M.L. (1976) A climatological spectral study of the 500 mb Geopotential height of the Northern Hemisphere. *Journal of the Atmospheric Sciences*, 33(8), 1607–1623.
- Dee, D.P., Uppala, S.M., Simmons, A.J., Berrisford, P., Poli, P., Kobayashi, S., Andrae, U., Balmaseda, M.A., Balsamo, G., Bauer, P., Bechtold, P., Beljaars, A.C.M., van de Berg, L., Bidlot, J., Bormann, N., Delsol, C., Dragani, R., Fuentes, M., Geer, A.J., Haimberger, L., Healy, S.B., Hersbach, H., Hólm, E. V., Isaksen, I., Kållberg, P., Köhler, M., Matricardi, M., McNally, A.P., Monge-Sanz, B.M., Morcrette, J.-J., Park, B.-K., Peubey, C., de Rosnay, P., Tavolato, C., Thépaut, J.-N. and Vitart, F. (2011) The ERA-interim reanalysis: configuration and performance of the data assimilation system. *Quarterly Journal of the Royal Meteorological Society*, 137(656), 553–597.
- Dee, D.P., Balmaseda, M., Balsamo, G., Engelen, R., Simmons, A.J. and Thépaut, J.-N. (2014) Toward a consistent reanalysis of the climate system. *Bulletin of the American Meteorological Society*, 95(8), 1235–1248.
- Enfield, D.B., Mestas-Núñez, A.M. and Trimble, P.J. (2001) The Atlantic multidecadal oscillation and its relation to rainfall and river flows in the continental U.S. *Geophysical Research Letters*, 28(10), 2077–2080.
- Feser, F., Barcikowska, M., Krueger, O., Schenk, F., Weisse, R. and Xia, L. (2015) Storminess over the North Atlantic and northwestern Europe—a review. *Quarterly Journal of the Royal Meteorological Society*, 141(687), 350–382.
- Gardiner, B., Blennow, K., Carnus, J.-M., Fleischer, P., Ingemarsson, F., Landmann, G., Lindner, M., Marzano, M., Nicoll, B., Orazio, C., Peyron, J.-L., Reviron, M.-P., Schelhaas, M.-J., Schuck, A., Spielmann, M. and Usbeck, T. (2010) *Destructive Storms in European Forests: Past and Forthcoming Impacts*. Cestas, France: Technical report. European Forest Institute.
- Gregow, H., Jylhä, K., Mäkelä, H.M., Aalto, J., Manninen, T., Karlsson, P., Kaiser-Weiss, A.K., Kaspar, F., Poli, P., Tan, D.G. H., Obregon, A. and Su, Z. (2016) Worldwide survey of awareness and needs concerning reanalyses and respondents views on climate services. *Bulletin of the American Meteorological Society*, 97(8), 1461–1473.
- Gregow, H., Laaksonen, A. and Alper, M.E. (2017) Increasing large scale windstorm damage in western, central and northern European forests, 1951–2010. *Scientific Reports*, 7, 46397.
- Gregow, H., Rantanen, M., Laurila, T.K. and Mäkelä, A. (2020) *Review on winds, extratropical cyclones and their impacts in northern Europe and Finland*. Helsinki, Finland: Technical report. Finnish Meteorological Institute, Reports 2020, p. 3.
- Hersbach, H., Bell, B., Berrisford, P., Hirahara, S., Horányi, A., Muñoz-Sabater, J., Nicolas, J., Peubey, C., Radu, R., Schepers, D., Simmons, A., Soci, C., Abdalla, S., Abellan, X., Balsamo, G., Bechtold, P., Biavati, G., Bidlot, J., Bonavita, M., De Chiara, G., Dahlgren, P., Dee, D., Diamantakis, M., Dragani, R., Flemming, J., Forbes, R., Fuentes, M., Geer, A., Haimberger, L., Healy, S., Hogan, R.J., Hólm, E., Janisková, M., Keeley, S., Laloyaux, P., Lopez, P., Lupu, C., Radnoti, G., de Rosnay, P., Rozum, I., Vamborg, F., Villaume, S. and Thépaut, J.-N. (2020) The ERA5 global reanalysis. *Quarterly Journal of the Royal Meteorological Society*, 146(730), 1999–2049.
- Hewson, T. (2020) *Use and Verification of ECMWF Products (2019)*. Reading, UK: Technical report. ECMWF Technical Memoranda.
- Howard, T. and Clark, P. (2007) Correction and downscaling of NWP wind speed forecasts. *Meteorological Applications*, 14(2), 105–116.

- Hurrell, J.W. (1995) Decadal trends in the North Atlantic oscillation: regional temperatures and precipitation. *Science*, 269 (5224), 676–679.
- Ionita, M., Lohmann, G., Rimbu, N., Chelcea, S. and Dima, M. (2012) Interannual to decadal summer drought variability over Europe and its relationship to global sea surface temperature. *Climate Dynamics*, 38(1–2), 363–377.
- Kaiser-Weiss, A.K., Kaspar, F., Heene, V., Borsche, M., Tan, D.G. H., Poli, P., Obregon, A. and Gregow, H. (2015) Comparison of regional and global reanalysis near-surface winds with station observations over Germany. *Advances in Science and Research*, 12(1), 187–198.
- Kaiser-Weiss, A.K., Borsche, M., Niermann, D., Kaspar, F., Lussana, C., Isotta, F.A., van den Besselaar, E., van der Schrier, G. and Undén, P. (2019) Added value of regional reanalyses for climatological applications. *Environmental Research Communications*, 1(7), 071004.
- Kaplan, A., Cane, M.A., Kushnir, Y., Clement, A.C., Blumenthal, M.B. and Rajagopalan, B. (1998) Analyses of global sea surface temperature 1856–1991. *Journal of Geophysical Research: Oceans*, 103(C9), 18567–18589.
- Kendall, M.G. (1970) *Rank Correlation Methods*. London: Griffin.
- Kiss, P. and János, I.M. (2008) Comprehensive empirical analysis of ERA-40 surface wind speed distribution over Europe. *Energy Conversion and Management*, 49(8), 2142–2151.
- Krueger, O., Feser, F. and Weisse, R. (2019) Northeast Atlantic storm activity and its uncertainty from the late nineteenth to the twenty-first century. *Journal of Climate*, 32(6), 1919–1931.
- Laapas, M. and Venäläinen, A. (2017) Homogenization and trend analysis of monthly mean and maximum wind speed time series in Finland, 1959–2015. *International Journal of Climatology*, 37(14), 4803–4813.
- Mann, H.B. (1945) Nonparametric tests against trend. *Econometrica*, 13, 245–259.
- Minola, L., Azorin-Molina, C. and Chen, D. (2016) Homogenization and assessment of observed near-surface wind speed trends across Sweden, 1956–2013. *Journal of Climate*, 29(20), 7397–7415.
- Minola, L., Zhang, F., Azorin-Molina, C., Pirooz, A.A.S., Flay, R.G. J., Hersbach, H. and Chen, D. (2020) Near-surface mean and gust wind speeds in ERA5 across Sweden: towards an improved gust parametrization. *Climate Dynamics*, 55(3), 887–907.
- Moore, G.W. and Renfrew, I.A. (2005) Tip jets and barrier winds: a QuikSCAT climatology of high wind speed events around Greenland. *Journal of Climate*, 18(18), 3713–3725.
- NOAA (2020a). www.cpc.ncep.noaa.gov/products/precip/CWlink/pna/nao.shtml. [Accessed: June 29, 2020].
- NOAA (2020b). www.esrl.noaa.gov/psd/data/timeseries/AMO/. [Accessed: June 29, 2020].
- Olauson, J. (2018) ERA5: the new champion of wind power modelling? *Renewable Energy*, 126, 322–331.
- Peings, Y. and Magnusdottir, G. (2014) Forcing of the wintertime atmospheric circulation by the multidecadal fluctuations of the North Atlantic Ocean. *Environmental Research Letters*, 9(3), 034018.
- Priestley, M.D.K., Ackerley, D., Catto, J.L., Hodges, K.I., McDonald, R.E. and Lee, R.W. (2020) An overview of the extratropical storm tracks in CMIP6 historical simulations. *Journal of Climate*, 33(15), 6315–6343.
- Rex, D.F. (1950) Blocking action in the middle troposphere and its effect upon regional climate. *Tellus*, 2(4), 275–301.
- Sampe, T. and Xie, S.-P. (2007) Mapping High Sea winds from space: a global climatology. *Bulletin of the American Meteorological Society*, 88(12), 1965–1978.
- Sandu, I., Zadra, A. and Wedi, N. (2017) Impact of orographic drag on forecast skill. *ECMWF Newsletter*, 150, 18–24.
- Scaife, A.A., Arribas, A., Blockley, E., Brookshaw, A., Clark, R.T., Dunstone, N., Eade, R., Fereday, D., Folland, C.K., Gordon, M., Hermanson, L., Knight, J.R., Lea, D.J., MacLachlan, C., Maidens, A., Martin, M., Peterson, A.K., Smith, D., Vellinga, M., Wallace, E., Waters, J. and Williams, A. (2014) Skillful long-range prediction of European and North American winters. *Geophysical Research Letters*, 41(7), 2514–2519.
- Sen, P.K. (1968) Estimates of the regression coefficient based on Kendall's tau. *Journal of the American Statistical Association*, 63 (324), 1379–1389.
- Sutton, R.T., McCarthy, G.D., Robson, J., Sinha, B., Archibald, A.T. and Gray, L.J. (2018) Atlantic multidecadal variability and the U.K. ACSIS program. *Bulletin of the American Meteorological Society*, 99(2), 415–425.
- Theil, H. (1950) A rank-invariant method of linear and polynomial regression analysis, 1–2. *Proceedings of the Royal Netherlands Academy of Sciences*, 53. 386–392 and 521–525.
- Thyness, V., Homleid, M., Køltzow, M. and Lien, T. (2017) *Application and Verification of ECMWF Products 2017*. Oslo, Norway: Technical report. Norwegian Meteorological Institute.
- Torralba, V., Doblado-Reyes, F.J. and Gonzalez-Reviriego, N. (2017) Uncertainty in recent near-surface wind speed trends: a global reanalysis intercomparison. *Environmental Research Letters*, 12 (11), 114019.
- Trocchi, A., Muller, K., Coppin, P., Davy, R., Russell, C. and Hirsch, A.L. (2012) Long-term wind speed trends over Australia. *Journal of Climate*, 25(1), 170–183.
- Tuononen, M., Sinclair, V.A. and Vihma, T. (2015) A climatology of low-level jets in the mid-latitudes and polar regions of the Northern Hemisphere. *Atmospheric Science Letters*, 16(4), 492–499.
- Usbeck, T., Waldner, P., Dobbertin, M., Ginzler, C., Hoffmann, C., Sutter, F., Steinmeier, C., Volz, R., Schneider, G. and Rebetz, M. (2012) Relating remotely sensed forest damage data to wind data: storms Lothar (1999) and Vivian (1990) in Switzerland. *Theoretical and Applied Climatology*, 108, 451–462.
- Vautard, R., Cattiaux, J., Yiou, P., Thépaut, J.-N. and Ciais, P. (2010) Northern Hemisphere atmospheric stilling partly attributed to an increase in surface roughness. *Nature Geoscience*, 3, 756–761.
- Vose, R.S., Applequist, S., Bourassa, M.A., Pryor, S.C., Barthelmie, R.J., Blanton, B., Bromirski, P.D., Brooks, H. E., DeGaetano, A.T., Dole, R.M., Easterling, D.R., Jensen, R.E., Karl, T.R., Katz, R.W., Klink, K., Kruk, M.C., Kunkel, K.E., MacCracken, M.C., Peterson, T.C., Shein, K., Thomas, B.R., Walsh, J.E., Wang, X.L., Wehner, M.F., Wuebbles, D.J. and Young, R.S. (2014) Monitoring and understanding changes in extremes: Extratropical storms, winds, and waves. *Bulletin of the American Meteorological Society*, 95(3), 377–386.

- Wu, J., Zha, J., Zhao, D. and Yang, Q. (2018) Changes in terrestrial near-surface wind speed and their possible causes: an overview. *Climate Dynamics*, 51, 2039–2078.
- Yamamoto, A. and Palter, J.B. (2016) The absence of an Atlantic imprint on the multidecadal variability of wintertime European temperature. *Nature Communications*, 7, 1–8.
- Zahradníček, P., Brázdil, R., Štěpánek, P. and Řezníčková, L. (2019) Differences in wind speeds according to measured and homogenized series in The Czech Republic, 1961–2015. *International Journal of Climatology*, 39(1), 235–250.
- Zecchetto, S. and Cappa, C. (2001) The spatial structure of the Mediterranean Sea winds revealed by ERS-1 scatterometer. *International Journal of Remote Sensing*, 22(1), 45–70.
- Zecchetto, S. and De Biasio, F. (2007) Sea surface winds over the Mediterranean Basin from satellite data (2000–04): Meso- and local-scale features on annual and seasonal time scales. *Journal of Applied Meteorology and Climatology*, 46(6), 814–827.
- Zeng, Z., Ziegler, A.D., Searchinger, T., Yang, L., Chen, A., Ju, K., Piao, S., Li, L.Z.X., Ciais, P., Chen, D., Liu, J., Azorin-Molina, C., Chappell, A., Medvigy, D. and Wood, E.F. (2019) A reversal in global terrestrial stilling and its implications for wind energy production. *Nature Climate Change*, 9, 979–985.
- Zhang, R., Sutton, R., Danabasoglu, G., Kwon, Y.-O., Marsh, R., Yeager, S.G., Amrhein, D.E. and Little, C.M. (2019) A review of the role of the Atlantic Meridional overturning circulation in Atlantic multidecadal variability and associated climate impacts. *Reviews of Geophysics*, 57(2), 316–375.

SUPPORTING INFORMATION

Additional supporting information may be found online in the Supporting Information section at the end of this article.

How to cite this article: Laurila TK, Sinclair VA, Gregow H. Climatology, variability, and trends in near-surface wind speeds over the North Atlantic and Europe during 1979–2018 based on ERA5. *Int J Climatol*. 2021;41:2253–2278. <https://doi.org/10.1002/joc.6957>